ADSORBENT SYNTHESIS FOR THE RECOVERY OF LITHIUM FROM WATER RESOURCES

A Thesis Submitted to
the Graduate School of Engineering and Sciences of
İzmir Institute of Technology
In Partial Fulfillment of the Requirements for the Degree of

MASTER OF SCIENCE

in Chemical Engineering

by
Anıl KAHVECİOĞLU

December 2022
İZMİR

ACKNOWLEDGEMENTS

I would like to send my heartfelt gratitude to my supervisor Assoc. Prof. Dr. Aslı YÜKSEL ÖZŞEN for his invaluable advise, encouragement, wide expertise, limitless empathy, and support throughout my graduate program.

I also grateful to Yaşar Kemal RECEPOĞLU for his comprehension and counseling especially with laboratory experiments.

Special thanks to Bahriyenur ARABACI and Fatih KIZIL for their endless support in the experiments, friendship, and hospitality.

Many thanks to Bekir Fırat ALTINBAŞ for his helpful contributions on very limited time and Ceren ORAK for giving valuable advice and profound belief in my work.

In these three years lots of things happened in my life and in the world. Because of this I am really thankful to our institute, professors, and my classmates to get through the hard times because of coronavirus.

Above all, I wish to express my most heartfelt thanks to my dearest parents and my brother for their unconditional love, continuous support, and encouragement throughout my life.

Last but not least I would like to thank myself for believing in me, for doing all this hard work, for never quitting, always being a giver and trying to give more than receive, for trying to do more right than wrong and being me at all times.

ABSTRACT

ADSORBENT SYNTHESIS FOR THE RECOVERY OF LITHIUM FROM WATER RESOURCES

Lithium is a crucial mineral for the 21st century due to its utilization in a wide range of industries. Lithium demand will increase because of car battery developments and the necessity for power storage. Investigating alternative strategies for resource recovery is the only way to fulfill this unexpected rise properly and sustainably in demand. Adsorption has been discovered to have some technological advantages over other methods. It is considerably less expensive, lacks the chemical resistance present in membranes, lacks the significant electrical demand of electrochemical approaches, as well as the restricted selectivity and challenges in integration into commercial processes. Lithium manganese oxides, also known as lithium ion-sieves, are adsorbents for lithium extraction that have remarkably high selectivity, high adsorption capacity, minimal toxicity, good chemical stability and cheap cost. They are one of the most promising inorganic adsorbents.

This research emphasized on the recovery of lithium from water resources through the use of lithium manganese oxide, which were synthesized in laboratory. They were transformed into spherical beads by adding chitosan, followed by crosslinking these beads with epichlorohydrin to increase their adsorption yield, stability, and reusability. Characterization techniques such as SEM, XRD and BET were applied on the adsorbents. Results shows that the adsorbents distributed uniformly, the adsorbent powder was mesoporous, and from the adsorption studies it was found that the adsorbent worked much better in alkaline conditions such as pH 12, optimum adsorbent dosage estimated as 4 g/L and the equilibrium time measured as 10 hours. From the desorption study approximately 95% of Li desorbed for the first cycle, after the second cycle the adsorbent efficiency started to decrease.

Keywords: *Lithium Recovery, Lithium Manganese Oxide, Adsorption*

ÖZET

SU KAYNAKLARINDAN LİTYUM GERİ KAZANIMI İÇİN ADSORBAN SENTEZLENMESİ

Lityum, çeşitli endüstrilerde kullanımı nedeniyle 21. yüzyıl için çok önemli bir mineraldir. Araç akülerinin üretimi ve enerji depolama ihtiyacı lityuma olan talebin artmasına neden olmuştur. Kaynak geri kazanımı için alternatif stratejiler araştırmak, talepteki bu beklenmedik artışı doğru ve sürdürülebilir bir şekilde karşılamanın tek yoludur. Bu araştırmalar sonucu adsorpsiyonun diğer yöntemlere göre bazı teknolojik avantajları olduğu keşfedilmiştir. Bunlar önemli ölçüde daha ucuz olması, membranlarda bulunan kimyasal dirençten yoksunluğu, sınırlı seçiciliği ve endüstriyel proseslere entegrasyon zorluğunun olmaması ve elektrokimyasal tekniklerdeki gibi aşırı elektrik gereksiniminden yoksun olmasıdır. Lityum iyon elekleri olarak adlandırılan lityum manganez oksitler, lityumun çıkarılması için alışılmadık derecede yüksek seçiciliğe ve kapasiteye, düşük toksisiteye, düşük maliyete ve güçlü kimyasal kararlılığa sahip adsorbanlardır ve dolayısıyla en umut verici inorganik adsorbanlardan biridir.

Bu araştırmada, lityum manganez oksit kullanılarak su kaynaklarından lityumun geri kazanılması çalışılmıştır. Bunun için laboratuvarda sentezlenen ve daha sonra kitosan katılarak küresel boncuklara dönüştürülen ve ardından bu boncukların epiklorohidrin ile çapraz bağlanması ile adsorpsiyon verimlerinin, stabilitelerinin ve tekrar kullanılabilirliklerinin arttırılması üzerinde durulmuştur. Adsorbanlar üzerinde yapılan SEM, XRD ve BET gibi karakterizasyon teknikleri sonucunda adsorbanların üniform olarak dağıldığı ve toz haldeki adsorbanın mezogözenekli olduğu görülmektedir. Adsorpsiyon çalışmalarında adsorbanın pH 12 gibi alkali koşullarda daha verimli çalıştığı ve optimum miktarın adsorpsiyon için 4 g/L olduğu bulunmuştur ve denge süresi 10 saat olarak ölçülmüştür. Desorpsiyon çalışmasının ilk döngüsünde lityumun yaklaşık %95'i geri kazanılmıştır, ancak ikinci döngüden sonra adsorban etkinliği hızla düşmüştür.

Anahtar Kelimeler: *Lityum Geri Kazanımı, Lityum Manganez Oksit, Adsorpsiyon*

TABLE OF CONTENTS

LIST OF FIGURES

LIST OF TABLES

CHAPTER 1

INTRODUCTION

Lithium is a crucial element that is used at different industries in 21st century (Siekierka 2020). Lithium and compounds that contains lithium are critical key assets for the economy and national defense, owing to that, the annual consumption is rising quickly. Lithium resources are currently mostly extracted from brines from salt lakes and solid minerals. In recent years, salt lakes and other terrestrial brine resources have provided more than 80% of the world's lithium products. Terrestrial brine supplies, however, are unable to meet long-term demands because of the high-tech industries' explosive growth, particularly in the aerospace, nuclear power, and energy conversion sectors (Xing et al. 2019). Due to the growing need for green technology and low-carbon emission economy, lithium has recently been added to the list of critical raw minerals prepared by European commission. (Alessia et al. 2021). Currently, a number of methods, including solvent extraction, solar evaporation, adsorption, co-precipitation, and membrane technologies, have been utilized for the lithium-ion recovery from water resources. Evaporative crystallization and precipitation, however, are only effective at low Mg to Li ratios and major concentrations of Li^+. Although extraction by solvent has been extensively studied for the lithium ion recovery from brines with higher Mg to Li ratios, its application is frequently constrained using organic solvents because of environmental issues. Ion exchange adsorption is the best option for recovering low concentrations of Li^+ from geothermal water for all these reasons (H. Wang et al. 2020). Due to their superior lithium-ion selectivity, ion-exchange adsorption techniques along with lithium-ion sieves have received the great attention among these techniques (S. Wang et al. 2018).

Lithium manganese oxides are one type of lithium ion-sieve adsorbents with unusually great chemical stability, low cost, low toxicity, good selectivity, and capacity for extracting lithium from water resources (Zhu et al. 2014). However, because the majority of lithium ion-sieves present in powder form, for that reason usage in industry is restricted because of a greater pressure drop, powder loss, and high energy consumption in column operation. To fill this gap, membranization, foam, and

granulation have historically been employed. In a variety of industrial applications, chitosan, a hydrophilic, biodegradable, and anti-bacterial substance, is frequently utilized for granulation (Vanessa L. Gonçalves, n.d.). Chitosan's functional groups and type of the crosslinker agent have the biggest effects on the crosslinking reaction. Since diffusion is made simpler by the crosslinker's reduced molecular size, the crosslinking reaction proceeds more quickly. The primary interactions constituting the network are covalent or ionic bonds, depending on the crosslinker's nature (Vanessa L. Gonçalves, n.d.). Epichlorohydrin, often known as ECH, is an epoxide and an organochlorine substance. It is a colorless liquid with a strong, garlic-like odor that is miscible with the majority of polar organic solvents but only mildly soluble in water used as a crosslinker.

This study focused on the utilization of lithium manganese oxide, which was synthesized in laboratory, to recover lithium from water resources. after adding chitosan, which turned them into spherical beads. These beads were then crosslinked with epichlorohydrin to improve their characteristics such as adsorption yield, stability, and reusability. They were finally prepared to collect lithium from water resources after delithiating with hydrochloric acid.

CHAPTER 2

BACKGROUND INFORMATION

2.1. Lithium

Lithium is an essential substance for this century and used in numerous sectors of industry such as a chemical substance, as a catalyst for polymerization, in high-performance glass and ceramics, as an enabling agent, among other relevant applications (Alessia et al. 2021). Additionally, lithium's outstanding characteristics, such as the low molecular weight (6.431 g/mole) and weak standard potential (-3.045 V), make it ideal for long-lasting battery packs used in small and light electrical components (Siekierka 2020). The chemical properties of lithium element were given in Figure 1.
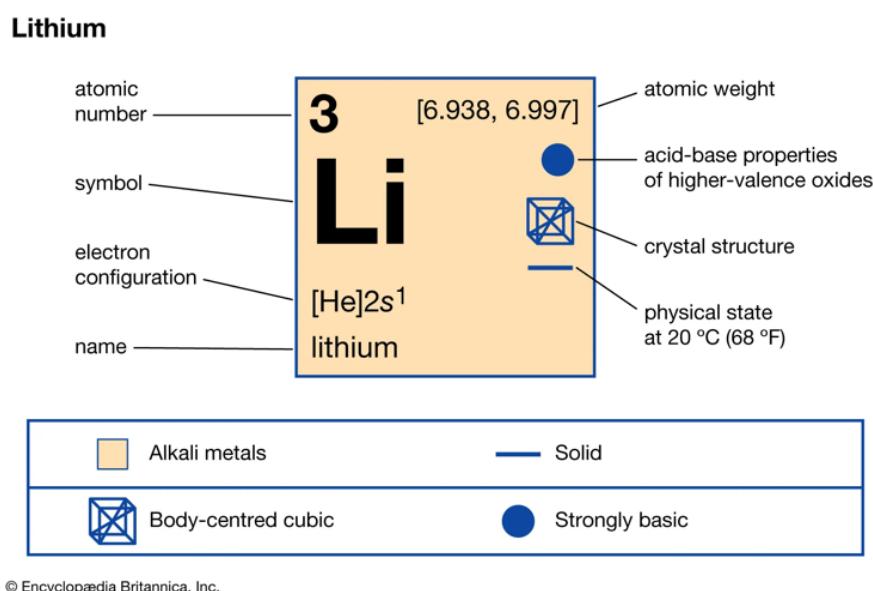
Figure 1. Chemical Properties of Lithium Element

This lightest alkali metal is used extensively in a wide range of activities, including electrode welding, air conditioning, thermonuclear fusion, ceramic glasses, rechargeable batteries, dyes, pharmaceuticals, lubricant greases, cements, and adhesives. Lithium market demand per year given in Table 1 below and lithium applications are given in Figure 2. Recently, the lithium demand in market has increased, whereas the availability of lithium deposits on land has significantly decreased (Xu et al. 2016). For instance, according to the International Energy Agency

(IEA), by 2040, the clean energy sector alone will consume four times as much lithium, nickel, and graphite (Khalil et al., 2022).

Table 1. The Lithium Market Globally, Most used sectors (Alessia et al. 2021)

Use Areas of Lithium	Demand of Lithium (Tonnes/Year)
Rechargeable Batteries	42200
Not Rechargeable Batteries	1500
Glass	2300
Ceramics	7000
Greases	7000
Air Treatment	1500
Metallurgical Powder	2300
Ceramics	7800
Polymer	3100
Other	5500

Investigation of critical raw materials (CRM) important to the economy of European union was listed as a primary task for the 2008 initiative. Resulting the first critical raw material list identifying 14 materials were issued in year 2011 following the evaluation of 41 non-agricultural and non-energy raw materials, based on an analysis of two important properties: the risk of supply also the importance in the economy which can be explained by primary supply concentration of countries that produced the raw material and the end-use applications which are adding value to the European Union respectively. Due to these reasons lithium has become one of the materials that was chosen and was thought to be on the edge (Alessia et al., 2021). In United States (US) federal law first used the term "critical material" in 1939 to refer to resources that are crucial for military, industrial, and basic civilian needs but cannot be obtained or manufactured in sufficient numbers in the US (Alessia et al. 2021).

Global Lithium end-uses
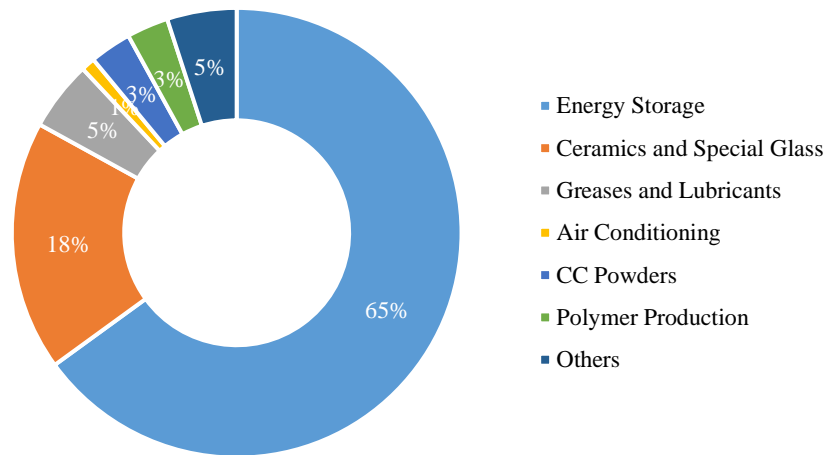
Figure 2. Percentage of Li end-uses worldwide in 2019 across numerous applications

Considering the requirement for energy storage and the manufacturing of vehicle batteries will cause lithium demand increase by up to 18 times in 2030 and 60 times in 2050. The only way to meet this sudden increase in demand satisfactorily and sustainably is to investigate alternate methods of resource recovery. In the past two decades, the price of lithium metal rises almost 10 times due to this fast demand (Khalil et al. 2022). From primary resources lithium extracted as lithium carbonate (Li_2CO_3), which has been broadly used as a pharmaceutical, for lithium-ion batteries' cathode material, and to lower the boiling point in applications involving glass and ceramics, as well as to boost thermal expansion resistance. The distribution of lithium resources in the world shown in Figure 3, which are primarily found in South America, results in a heavy reliance on imports for this material in Europe, which is another crucial factor in the assessment of supply risk.(Zavahir et al. 2021) Since the amount of lithium already collected is negligible, enormous efforts should be done to prevent criticality.

2.2. Sources of Lithium

Lithium is largely gathered from two main sources: mineral ores of lithium, such as petalite and spodumene ores, and lithium water sources, such as sea water, salt-lake brines, and geothermal water (Xu et al. 2016). According to Figure 3 distribution of lithium resources worldwide can be observed (Xu et al. 2016).
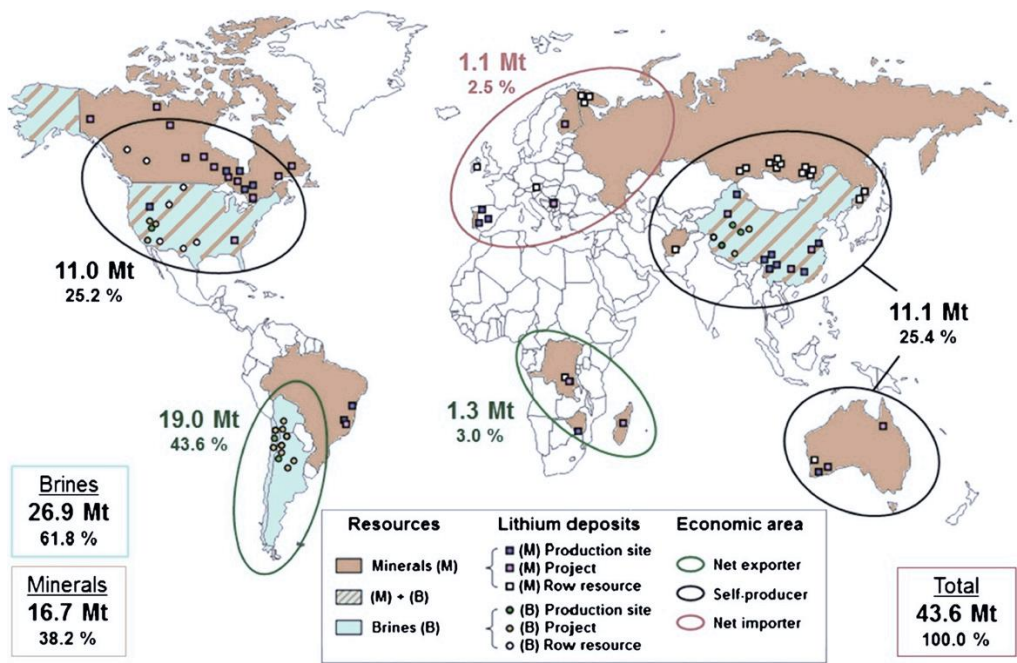
Figure 3. Lithium resource availability in worldwide map

Reservoirs of water have the biggest amounts of lithium compounds. According to studies, there are 2.5×10^{14} kg of lithium ions in the world's water sources which are tabulated in Figure 4 and Figure 5. Li^+ ion average concentration distributed as 0.17 ppm, between 0.1 to 0.2 mg/dm^3 and 15 mg/L in seawater, groundwater, and geothermal water respectively (Siekierka 2020).
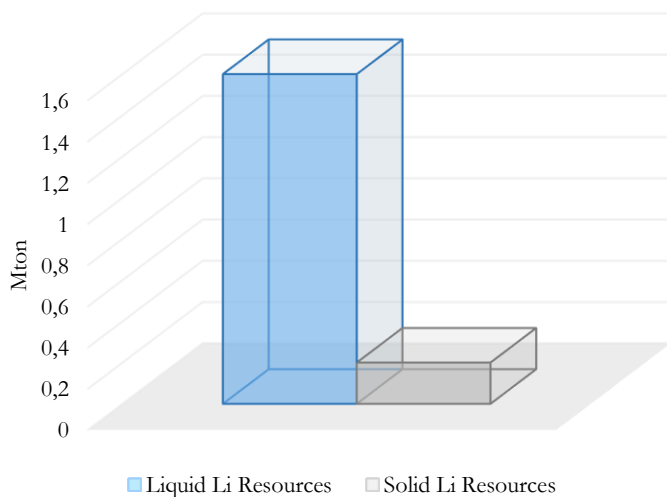
Figure 4. Liquid and Solid Lithium Resources Distribution through the World in Mton

Lithium is collected from mineral deposits in the earth and also precipitated from brine. But since there aren't many Li-based minerals, there will inevitably be a

requirement for future additional Li^+ sources (H. J. Hong et al. 2013). Currently, the two main minerals used on a commercial basis for Li extraction are Li carbonate and Li hydroxide (Khalil et al. 2022).
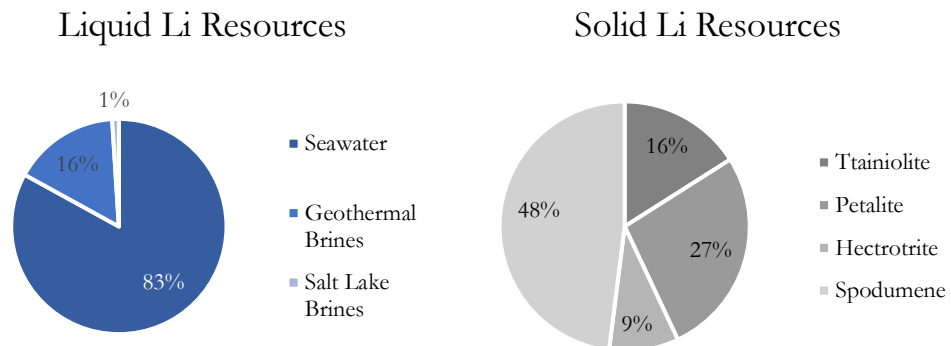
Figure 5. Based on their physical state, the quantity, and types of lithium resources

Geothermal brine is used as a secondary source of lithium, because of its smaller volume and integration into its use in the production of power (Ighalo et al. 2022). Geothermal fluids that have rich lithium compositions are gaining attention because they can be a source of green energy. Geothermal water contains lithium at levels as high as 10 mg/L. Benefits of the geothermal water are low ratio of Mg/Li and solids which are totally dissolved make it a potential liquid lithium mineral resource.

2.3. Lithium Recovery Methods

The recovery of lithium has attracted a lot of attention recently (Zhao et al. 2022). Numerous techniques for lithium recovery from seawater and brines have been used such precipitation, adsorption, solvent extraction, and membrane technologies (S. Wang et al. 2018). The solar evaporation method, which involves many steps to precipitate and Mg(OH), NaCl, $MgCO_3$, and Li_2CO_3 compounds turned to crystal, is the most often used. The brines must first be concentrated, which takes many months, and the produced Li_2CO_3 is blended with various minerals like magnesium salts (Xu et al. 2016).

In precipitation technique, metal sulphides or hydroxides can directly precipitate out of the geothermal water. This procedure, however, is solely appropriate when the metal concentration is low, and the metal variety is not vast. If there are several different types of metals present, the precipitate turns into metal sulphide complex that needs additional process, which raises the duration and cost of production. Precipitation would

likewise be ineffective if the metal concentration is higher above the threshold for solubility (Cetiner et al. 2015).

Co-precipitation technique is an alternate technique that produces lithium aluminum hydroxide by first adding agents like $AlCl_3$ to brines and then adjusting the pH with caustic alkali.

In bioaccumulation, Li can be taken up from geothermal water, which uses reaction of biochemical mediation processes in cells which are vital. Redox reaction and sulfate reduction are the main mechanisms. It differs significantly from biosorption process, which involves the bulk absorption plus surface uptake of dead cells that are both of plant and animal origin. (Recepoğlu et al. 2018).

Another technique, called solvent extraction, recovers Li^+ in the existence of different ions in liquid solutions with the help of chelating agent dipivaloylmethane (Xu et al. 2016). However, nanofiltration and electrically switched ion exchange technologies typically need the usage of expensive membranes, whilst high concentrations of lithium are primarily useful for recovery with the evaporative crystallization and solvent extraction procedures (Zhao et al. 2022). A low-cost method for recovering different chemical compounds from the aqueous phase is adsorption. Li uptake via ion-exchange with membranes or resins (instead of adsorbents) can be a costly method and this method is highly pH sensitive. The hydration radius, molecular structure, and electric charge of the resin all have a significant impact on its selectivity. Membranes may also be useful for recovering Li. Following separation, membranes keep the soluble salts and metals in the liquid media chemically pure, simplifying any subsequent processing that may be necessary. They are also more expensive because of the high-pressure usage and the resistance of chemicals (Ighalo et al. 2022). Adsorption is considered one of the most promising approaches, however it is still very difficult to produce adsorbents with excellent adsorption performance and stability (Zhao et al. 2022).

These Li recovery techniques also present some unique sustainability difficulties. Massive quantities of organic solvent and ionic liquid waste from solvent extraction raise significant environmental issues (Khalil et al. 2022).

2.4. Adsorption Mechanism of Li

It is required to get over the obstacles and limitations of the traditional brine disposal and treatment technologies. Numerous studies have been investigated the function of adsorption as a technique for recovering contaminants and valuable resources from brine solutions (Panagopoulos et al., 2019; Lakherwal, 2014). One of the most popular methods, adsorption is used for removing specific contaminants and targeted chemicals from brine solutions and wastewater because it is effective, economical, and selective. With flexibility in design and operation, the full recovery of minerals from brine can be accomplished. An adsorbent which is a solid material, used in the adsorption process, to capture the target substance (adsorbate) on its surface as can be seen from Figure 6. Additionally, the adsorbate often forms chemical or physical bonds with the adsorbent surface.
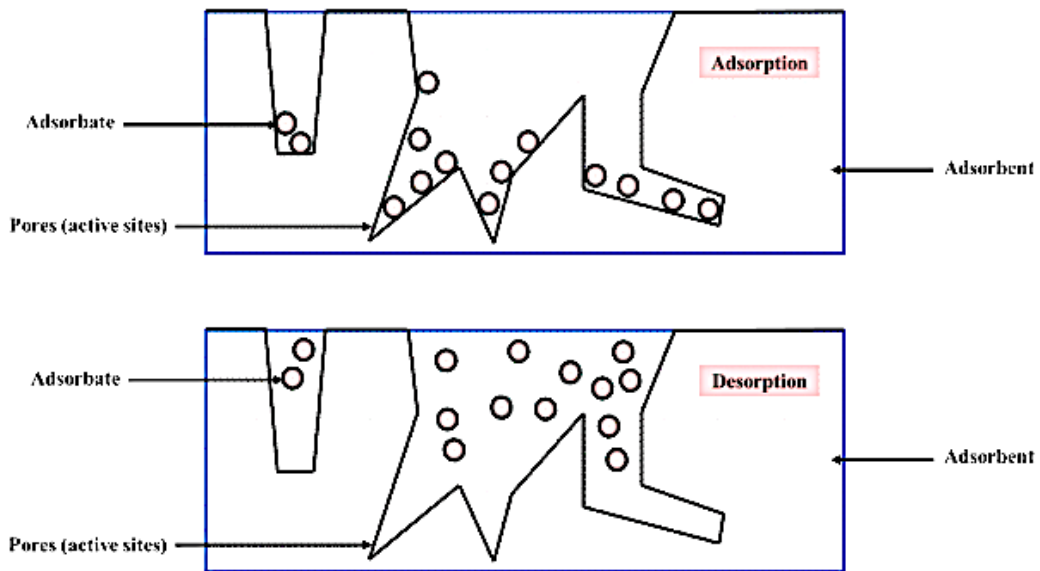
Figure 6. Adsorption/Desorption diagram, flow of adsorbed molecules into the adsorbent's active sites

When the adsorbate and the adsorption surface are brought together by covalent bonds, chemical bonding occurs. Moreover, when intermolecular bonding predominate, physical connection occurs among the adsorbate and adsorbent. The capacity of adsorption (q_e) of adsorbent is the adsorbate dosage it can hold per unit mass. To enhance the effectiveness of the adsorbent, maximizing capacity of adsorption can be

9

considered. Typically, a mathematical formula (*Eq.1*) was employed to compute and determine the adsorption capacity.

$$q_e = \frac{(C_i - C_e)\, V}{m} \qquad\qquad Eq.1$$

where C_i is initial, and C_e is equilibrium concentrations for the metal ion's in (ppm). Volume of solution (V) is given in liters (L), and the mass of adsorbent material was given in grams (g). It is possible to remediate or recover important chemicals and metals from brine streams using traditional adsorbents including activated carbon, alumina, chitosan, ion-exchange resins, zeolites, and silica gels. For their target pollutant, scientists typically choose an adsorbent due to its affordability, selectivity, usability, ease of access, stability, adaptability, capacity to regenerate, and high surface area.

It has been found that adsorption has some technological advantages over other techniques. It is significantly less expensive, lacks the chemical resistance seen in membranes, lacks the restricted selectivity and challenge of industrial process integration, and lacks the extreme electricity need in electrochemical approaches. The distribution and concentration of the ionic agents in the solution can also be influenced by the type of the source rock. This indicates that lithium and other cations are always competing for empty sites on adsorbent surface (Ighalo et al. 2022). The conventional lithium-ion sieve for lithium extraction method hasn't seen much popularity in industry during the past few decades.

One of the main reasons why the Li adsorption and desorption cycle is usually unfeasible is the time it needs to reach equilibrium. In principle, there are two main issues that are limiting the effectiveness of lithium recovery: minimal rates of Li^+ diffusion in aqueous medium and low rates of lithium-ion exchange in adsorbent particles. By raising the adsorption temperature, initial solution pH, and lithium content in the   solution, the first method can be made better (Xu et al. 2016).

2.4.1. Ion Exchange And Sorption

Due to their cheap cost and high efficiency, ion-exchange techniques are gaining popularity as "Li sieves", LIS, exhibit remarkable selectivity toward Li ions. Furthermore, LIS works even with low Li concentrations, which are typical of most

brines that occur naturally. This technique entails the systemically creation of active sites on mesoporous materials that are exceptionally selective for Li ions. Lithium-ion sieves come in two varieties: titanium-type LIS and manganese-type LIS both of which are used to lithium ion adsorption from liquids containing lithium (S. Wang et al. 2018). Recently, lots of articles have been published about the capacity of manganese and titanium-based adsorbents to selectively remove Li from brine sources. Due to their exceptional lithium selectivity, outstanding regeneration performance, and high lithium absorption capacities, lithium manganese oxide type LIS's are currently the widely used selective lithium adsorbents. The LIS technology is regarded as one of the most promising among several aqueous recovery methods. Because of their strong selectivity to lithium, high lithium absorption capacity, and favorable performance cycle, LISs are excellent adsorbents. Studies on delithiated LIS made by acid treatment of Li-containing oxides have received a lot of attention. (Khalil et al. 2022).

Additionally, it is excellent for pollutant pickup at low and medium concentrations (Ighalo et al. 2022). Fine-powder adsorbents, however, cannot be used in water directly because a large quantity of them is difficult to manage in the water, and they also have a problem being recovered from the water after Li^+ adsorption. Additionally, it can be challenging to obtain powder adsorbent containment materials that are hugely water permeable without causing the powder to leach. Granulation of the adsorbent in powder form is necessary for practical applications to increase adsorbents mechanical properties (H. J. Hong et al. 2013). Lithium's high-efficiency extraction from aqueous solutions is stated to be made possible by the environmentally benign and promising technique of adsorption. This is important to create composite materials that are functional and have high selectivity for adsorption and performance for adsorption-desorption (Zhao et al. 2022). Electrostatic attraction, intermolecular and intramolecular complexation, intercalation with related hydrogen bonds, and other significant mechanisms were also noted (Ighalo et al. 2022).

2.4.1.1. Li ion Sieves

Ion exchange adsorption and other major techniques for recovering lithium ions from solutions are crucial in terms of price and effectiveness. LISs are a brand-new class of economical green lithium-ion adsorbents. They draw a lot of interest in the recovery of lithium from various solutions. This is largely related to the higher cycle performance, high lithium absorption capacity, and outstanding lithium selectivity. In comparison to

other traditional approaches, the process of lithium recovery also offers superior security, dependability, and high recovery performance. Since land-based lithium deposits are depleting, it is anticipated that LIS technologies to extract lithium from brines from salt lakes and seawater will advance. Undoubtedly, such advancements will lessen market pressure on lithium supplies around the world. It's noteworthy that when compared to raw LISs, the existing Lithium-ion storage methods (LIS) reduce lithium capacity and absorption efficiency. Therefore, future research should concentrate on developing better adhesives, improving lithium adsorbents, and enhancing the setting up of composite material formation conditions (Xu et al. 2016).

In addition, certain popular LIS composite material making techniques are also investigated. These processes include foaming, granulation, the creation of membranes and fibers, and magnetization. These techniques are employed to improve industrial column operations.
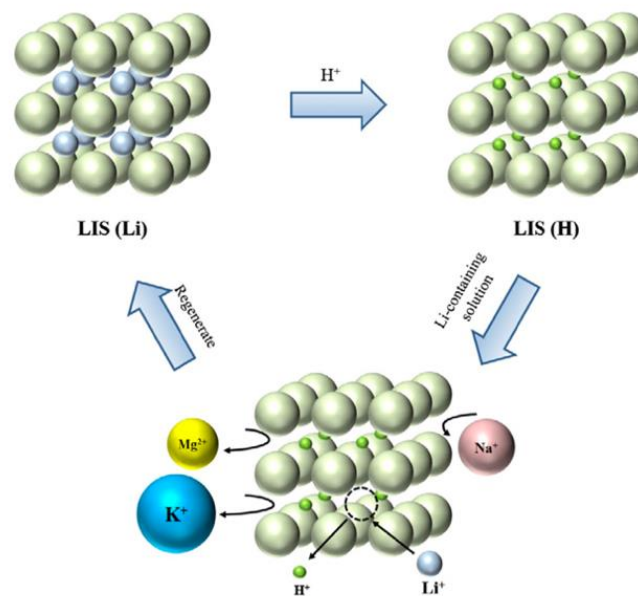
Figure 7. Representation of LIS Process

Ion-sieve oxides can be used for metal ion-screening effectively. These adsorbents are made using the proper precursors, which contain the desired metal ions. The predecessors frequently have consistent molecular structures, which allow the unoccupied crystal sites to be kept even after the target ions have been removed from their crystal locations. It was shown that, when the sieves are introduced to solutions that contain different types of metal ions, selective adsorption of lithium ions can be

achieved, as seen in Figure 7. The first stage is the generation of LIS with hydrogen loaded state [LIS (H)], which is accomplished by eliminating the lithium ions out from lithium loaded state [LIS (Li)], mostly through Li-H ion exchange. Following this, lithium ions in LIS are selectively adsorbed via the steric effect from solutions containing Li+. The utilized LIS (H) is then revived to create LIS by the adsorption of some lithium ions (Li). The entire procedure can be referred to as the "LIS effect." But the multiple valence states of manganese could lead to a range of lithium manganese oxides having different crystal shapes.

It is difficult to use LISs instantly for commercial column operation because they are often present in industrial applications as powder, which has, poor permeability, and poor recovery efficiencies. Also, the use of LISs in powder form during column operations can lead to large pressure decreases, powder loss, and energy consumption. Several methods, to change the form of the powdered adsorbents were proposed to change the form of LISs. Round beads, permeable foam, mixed matrix membrane, and ceramic granules are only a few examples of the composite adsorbents that have been created to address this issue (Zhao et al. 2022).

The solution's coexisting Na^+, Mg^{2+}, Mg2+, K^+, and Ca^{2+} ions had no effect here on LIS membrane adsorbent's high Li^+ selectivity. The lithium ion-sieve membranes are the most potential material for lithium ions in liquid lithium mixture due to its excellent resilience, good selectivity, and ease of use (Zhu et al. 2014).

Lithium manganese oxides considered to be the best adsorbent for extracting Li^+ from mixtures (H. J. Hong et al. 2013). Lithium manganese oxides, which are among the promising inorganic adsorbents, are lithium ion-sieves adsorbents with extraordinarily good selectivity and high capacity, moderate harm, cheap cost, and good chemical stability for lithium extraction from water sources (Zhu et al. 2014) . Three different chemical views are given in Figure 8. In order to produce millimeter-sized spherical particles that could be in a packed column without experiencing a significant pressure loss, granulation was accomplished by either utilizing polyvinyl chloride (PVC) as such binder or injecting ion-sieve powder inside macroporous beads (Zhu et al. 2014).
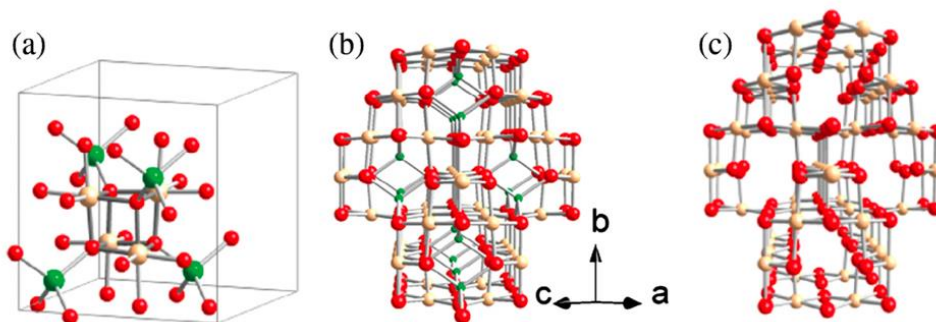
Figure 8. Three views of LiMn2O4 in perspective view(a), unit cell of spinel as the cubane core (b), framework structure as an extended three-dimensional.

There is still a lot of work to be done before these materials and synthesis techniques are applied on a broad scale because they are now based primarily on laboratory experiments. Adsorbents' chemical and thermal stability is crucial for many uses, particularly for Li^+ recovery from hot geothermal water (Zhao et al. 2022).

2.5. Chitosan

Chitin is converted into the natural polymer chitosan through the process of alkaline deacetylation. Following cellulose, chitin is the most prevalent biopolymer in nature.
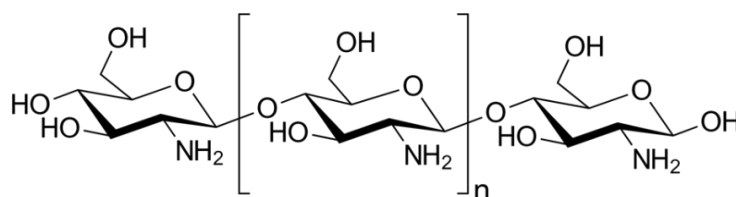
Figure 9. Chemical Representation of Chitosan

Chitosan is utilized as a food additive, a moisturizer in cosmetics and a drug component in biomedicines due to its low cost, biodegradability, nontoxicity, and hydrophilic nature. When used as a binding substance, chitosan's water permeability and hydrophilicity qualities are favorable. As seen from the Figure 9 the chemical representation contains NH_2 group. Unlike other natural polymers like PVA or PVC, plastics that are water-permeable can pass through water (H. J. Hong et al. 2013). However, high basic and acidic conditions are regularly encountered during the desorption and adsorption of Li^+ by LMOs, and under acidic conditions, chitosan would considerably dissolve. Because chitosan contains several hydroxyl and amino groups, cross-linking with various cross-linking reagents is frequently used to increase

chitosan's chemical stability (Zhu et al. 2014). The most popular technique for creating LISs adsorbent powders is granulation technology. By utilizing this technology, LISs might achieve high mechanical stability and excellent water permeability.

CHAPTER 3

LITERATURE SURVEY

The literature studies and comparison of the adsorbents will be reviewed in this section. Every article reviewed one by one, and their important sections will be mentioned.

In the study of Han et al. lithium manganese oxide in spinel type was processed using a combination of different methods, consisting of foaming, drop-in-oil, and agar gelation to create spherical, millimeter-sized ion-sieve foams (SIFs) and in difference of agar content seen in Figure 10, which were used for lithium extraction from untreated seawater. After being subjected to acid treatment, the spinel morphology of the produced SIFs was driven via H^+- Li^+ ion exchange, and such hierarchical trimodal porous structure of the SIFs was found. The elimination of the agar caused by the acid treatment resulted in the formation of various sizes in bimodal mesopores, and the bubble template produced macropores.
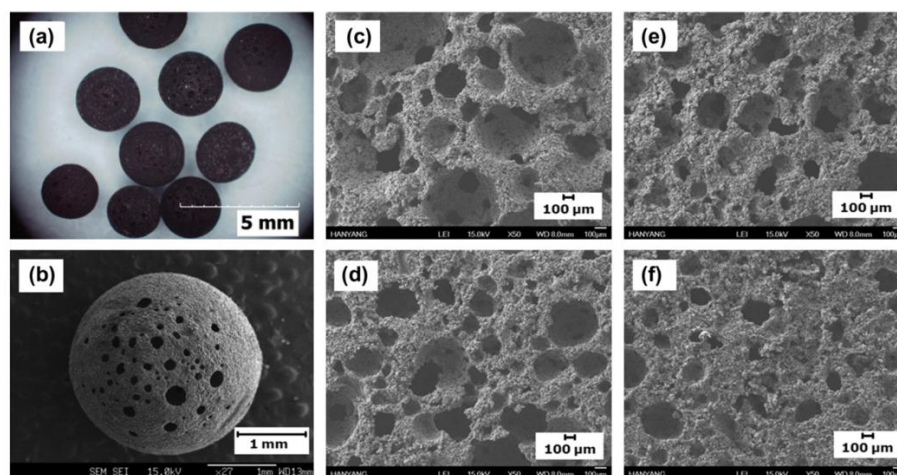
Figure 10. Surface morphology of SIFs made with various amounts of agar.

The SIFs' mesopore volume and an increase in the specific surface area as the amount of agar was increased was observed during the production process, but the macropore volume decreased which was properly shown in Figure 10 which corresponds to SEM pictures of the cross-sectional area (interior surfaces) of the SIFs with varying agar contents: 2% (a), 3% (b), 4% (c), and 6% (d) are shown alongside photographs of the SIFs (a), a full SIF (b), and a SEM image of a single SIF (f). With

more agars present throughout the process of production, the percentage of lithium adsorption inside the LiOH mixture considerably decreased. This is likely due to the sieve ion foam made with reduced agar content had extra open pores, increasing the likelihood that these pores would encounter the structure formed inside the interior of the sieve ion foams. The SIFs which have the reduced agar percentage had the highest capacity for lithium adsorption in natural seawater (3.4 mg/g), and even after fifth cycle of adsorption and desorption, the efficiency was almost unaffected. As the SIFs with various agar concentrations were submerged in 0.1 M LiOH with pH 13, solution at 25°C for a day, the lithium's adsorption ability was evaluated. When the lithium adsorption capabilities of LMO and HMO were compared, the identical conditions were applied to both materials. The highest lithium adsorption capacity was demonstrated by SIF-2 (20.9 mg/g), and the minimum (2.7 mg/g) by SIF-6. Lithium adsorption in HMO, which was previously created using the solid-state reaction method, was 24.1 mg/g, least than it was in spinel lithium manganese. Especially, this study's calculations showed that the lately reported spinel lithium manganese oxide's capacity of lithium adsorption, a class of powder ion- sieve, was greater than that of HMO. The SIFs with the lowest agar content (SIFs-2) adsorption of lithium in natural seawater was 3.4 mg/g, and after five adsorption-desorption cycles, the adsorption efficiency remained at over 95%. Five adsorption-desorption cycles later, the desorption efficiency was still at 86%. These findings imply that the millimeter-sized sieve ion foams are a good candidate for use in natural seawater as an ecologically friendly, semi-permanent lithium adsorbent (Han, Kim, and Park 2012).

From the article of Nisola et al. successful fabrication and evaluation of macroporous foam composites with polyvinyl alcohol (PVA) by high loadings of lithium-ion sieves (LIS) which are distributed uniformly for Li^+ recovery. Cryo-desiccation and surfactant blending efficiently created LIS/PVA foams with multilayered porosity made up of macro and mesopores and the preparation shown in Figure 11. The LIS/PVA foams were made water resistant by glutaraldehyde cross-linking, but they still had a significant water absorption capacity. As a result, when compared to the LIS powder, LIS/PVA foams with loading which around 200–300 weight percentage, showed only modest losses in q_e (7–13%) and kinetic characteristics. Selectivity of Li^+ through LIS/PVA foams against other cations, such as K^+, Na^+, Mg^{2+},

and Ca^{2+}, also increased as LIS loading increased and began to resemble that of the LIS powder.

Figure 11. LIS/PVA foam preparation with surfactant blending and cryo-desiccation combination in schematic diagram

LIS/PVA foams' Li^+ selectivity against other cations such K^+, Na^+, Mg^{2+}, and Ca^{2+}, also increased as LIS loading increased and began to resemble that of the LIS powder. Reducing the LIS loadings to 200 and 250-wt% were extremely robust and showed no degradation in performance of adsorption or reusability, in contrast to 300 wt.% LIS/PVA, which had weak mechanical property. The produced LIS/PVA with a 250-weight percent showed the best performance of adsorption and can be applied again over an extended period of time. It kept 91% of the q_e from the LIS powder, had high Li^+, successfully segregated Li^+, and concentrated Li^+ more than the other cations. The stated LIS/PVA foams could really be used for Li+ extraction from secondary sources because they don't require energy-intensive procedures such packed bed and membrane technologies (Nisola et al. 2015).

In the research of Park et al. produced, characterized, and evaluated $H_{1.6}Mn_{1.6}O_4$ (HMO) lithium ion-sieves with are composite with poly(acrylonitrile) (PAN) nanofibers for recovery of lithium ion. Nanofibers were produced via electrospinning 10 wt.% HMO/PAN doped mixtures in dimethylformamide with varied HMO loadings which can be seen from Figure 12. High-capacity composite nanofibers for absorbing water were found to be highly porous, physically, and chemically stable.
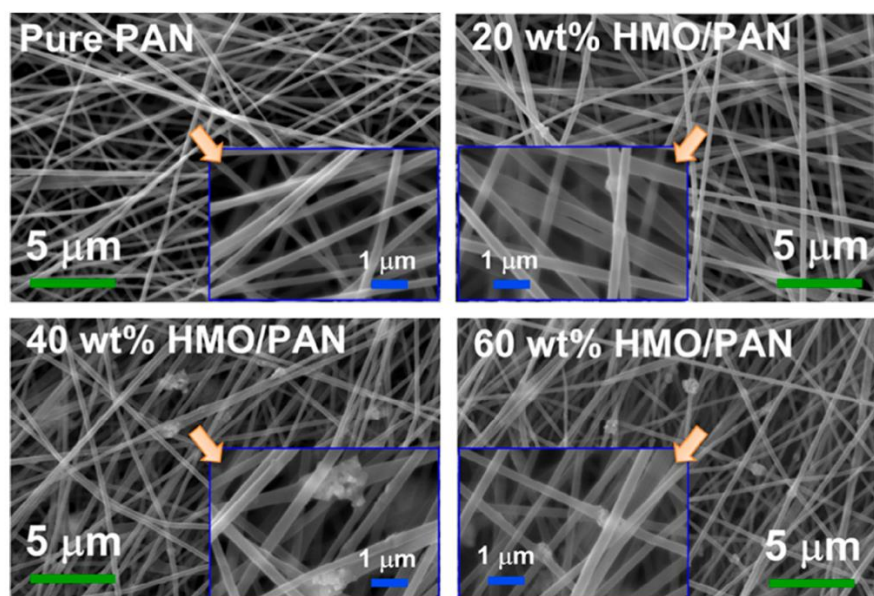
Figure 12. Various HMO loading of HMO/PAN with SEM images

Because HMO particle sizes and nanofiber diameters are similar (both are about 100 nm), PAN can be used as a binder with little interference from HMOs. Langmuir-type Li^+ adsorption was used by all of the evaluated adsorbents (q_m). Greater HMO loadings enhanced adsorption performance as more HMOs were exposed on the fiber surface and became less impacted by the binder; the greatest q_m=10.3 mg/g recorded with 60 wt% HMO/PAN was just 4% less than the support-free HMO. Loss in adsorption was only slightly affected (4%) after ten reuses, suggesting that HMO/PAN is stable over the long run. Li^+ was adsorbed preferentially by HMO/PAN with 60% loaded over other cations. in seawater desalination retentate, a high Li^+ distribution coefficient (K_D = 770). Li^+ was increased up to 486 times, but interfering cations were only enriched up to around 7. Overall findings show that the developed composite nanofiber HMO/PAN can be recycled and used to recover Li^+ from seawater or other potential sources. Since pH levels higher than 11 were shown to be the optimum for HMO powder Li^+ uptake, this pH level was chosen as the starting point for Li^+ solutions. Q_e gradually increased as the initial Li^+ concentration was raised before reaching its optimum amount of 10.8 mg/g at C_o = 35 mg Li^+/L.(Park et al. 2014)

Hong et al.'s research involved the creation of porous structure cylindrical HMO/Al2O3 composites and an analysis of their Li adsorption behavior in saltwater. For the manufacture of HMO/Al_2O_3 composites as illustrated in Figure 13, different ratios of lithium manganese oxide (LMO): alumina gel (1:4, 1:5, 1:9, 1:19, and 1:39)

were tried. Because mesoporous γ-Al_2O_3 has a large surface region, all LMO/Al_2O_3 composites have large surface areas. The surface area of the composite is increased, and a more porous structure is obtained by adding more Al_2O_3, whilst spinel phase of LMO's crystallinity is lowered. After delithiation, Li adsorption from saline was accomplished using the HMO/Al_2O_3 composite.
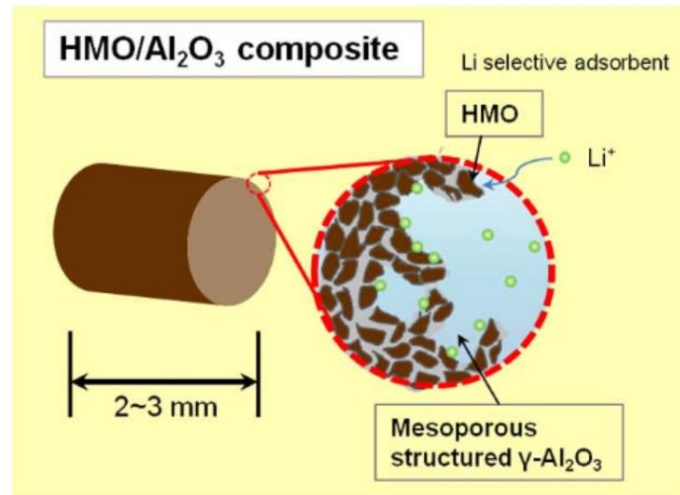
Figure 13. Illustration of HMO/Al_2O_3 composite

HMO/Al_2O_3 composites demonstrated significant Li absorption to hydrogen manganese oxide powder at about 9 mg Li/g HMO because of its significantly greater surface area also high porosity. Because of the low crystallinity of the spinel HMO, more manganese dissolution from materials contains greater amount of Al_2O_3 while recovering the adsorption of lithium ion onto the composites of HMO/Al_2O_3 by the means of treating with acidic solutions. The efficiency for Li adsorption did not degrade over the course of the five repetitions of Li adsorption-desorption, while HMO/Al_2O_3 with a 25% Al_2O_3 composition demonstrated less than 1% Mn dissolution. (H.-J. Hong et al. 2018)

From another research of Hong et al. they tried to efficiently recover Li^+ from seawater, on alpha-alumina beads, hydrogen manganese oxide (HMO) is immobilized (AABs). AABs are treated with calcination and acid after being dipped in a Li/Mn acetate solution to immobilize HMO on them and the appearance of the before and after can be seen from Figure 14. Li/Mn acetate solution concentration was adjusted from molarity of 2 to 8. Due to the AABs' small surface area, the quantity of HMO immobilized on them increased in direct proportion to the solution of Li/Mn acetate concentration, reaching saturation at 6 M. HMO loadings in the samples generated with

6 and 8 M solutions varied between 69.3 to 75.6 mg/cm^3 at their maximum. At the precursor concentration of Li/Mn was 2 M, HMO displayed the maximum adsorption performance of lithium ion (21.7 Li$^+$ mg/HMO g) in seawater that had been spiked with 30 mg/L Li$^+$. When taking into account the lithium-ion adsorption efficiency and the quantity of HMO immobilized on AAB, a 4 M Li/Mn precursor concentration resulted in the maximum amount of recovered lithium ion per volume.
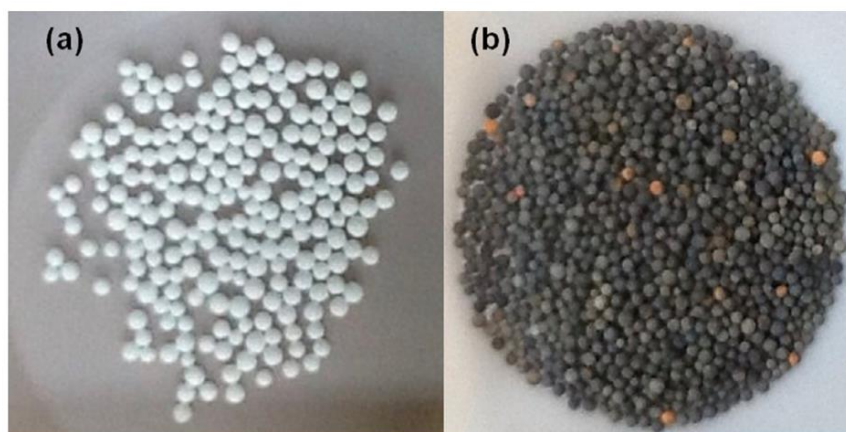
Figure 14. AAB (a) and HMO/AAB (b) pictures

Despite the low concentration of lithium ion in seawater, HMO immobilized to alpha alumina beads with 4 M Li/Mn precursor amount, demonstrated good lithium-ion adsorption capability (8.87 mg Li$^+$/g HMO). Because of improved saltwater interaction due to immobilization, HMO/AAB exhibits significantly better capability of lithium-ion adsorption than the power of hydrogen manganese oxide. After 14 cycles of adsorption and desorption for lithium ion, HMO immobilized on AAB still retained smaller than 2% of its fresh HMO's lithium-ion adsorption capability. This result demonstrates that lithium ion may be recovered from seawater by HMO immobilized on AAB (H.-J. Hong et al. 2015).

In the work of Koilraj et al, they used sodium alginate (AL) beads which are shown in Figure 15, lithium-ion sieve (HMO) powder made of uniformly integrated biogenic birnessite. The Li$^+$ adsorption characteristics of the composite beads were next investigated. Even after drying, the HMO parts were evenly scattered in the AL beads, according to a scanning electron microscopy-energy dispersive spectroscopy examination.
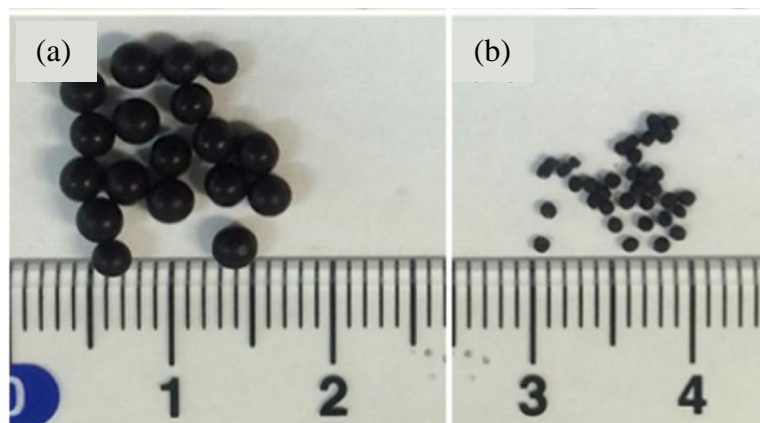
Figure 15. Size comparison of wet (a) and dry (b) HMO-AL beads

The linear Langmuir model accurately predicted the adsorption lithium ion to HMO isotherm contained in alginate beads (HMO-AL), and the beads' maximal hydrogen manganese oxide adsorption rate was 3.61 mmol/g, which is proportional to the rate of the original powdered HMO. For the initial lithium-ion concentration range from 2.56 to 4.23 mM, kinetic studies showed that Li^+ adsorption follows a model of pseudo-second order with rate constant $k_2 = 2.8$-$11.9x10^{-3}$ g/ (mmol min). The diffusion of lithium ion from aqueous medium to the HMO particle through to the Ca-AL network is the rate-limiting step for the adsorption of Li^+ on HMO-AL beads. The HMO-AL beads improved the handling effectiveness for Li^+ adsorption and allowed for several reuses without noticeably reducing Li^+ adsorption effectiveness (Koilraj et al. 2016)

From the article of Moazeni et al, they used ion exchange procedure for removing lithium from brine and saltwater that contain only small amounts of lithium. To accomplish this, it is crucial to use an adsorbent that has high adsorption capacity with the best potential for lithium adsorption along with a stable shape during the operation. In this work, a straightforward two-step hydrothermal procedure was used to make lithium titanate spinel with a nanotube shape, then titanium dioxide. A diluted acidic solution was then applied to the created $Li_4Ti_5O_{12}$ spinel ternary oxide nanotubes, which had a diameter of 70 nm, to prepare a brine-based adsorbent suitable for lithium adsorption.
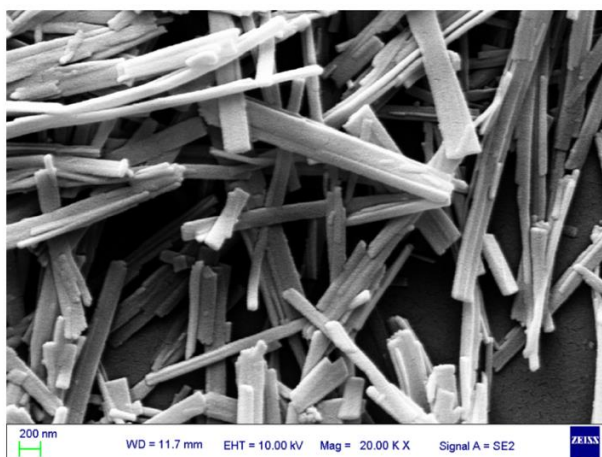
Figure 16. Titanium ion sieve FE-SEM image

The produced nanostructured materials' morphology and phase were examined using X-ray diffraction, transmission and scanning electron microscopes and other techniques, scanning electron microscopy image was shown in Figure 16. This adsorbent's ability to exchange lithium ions was ultimately assessed using an adsorption isotherm. The outcomes demonstrated that titanium dioxide adsorbent could extract 39.43 mg/g of the lithium, in 120 mg/L of lithium solution (Moazeni et al. 2015).

From another research of Hong et al., lithium (Li) recovery from saltwater has been the subject of much research into the compound hydrogen manganese oxide (HMO). A granular HMO must be acquired for a practical use. However, the performance of Li adsorption is reduced due to seawater diffusion being hampered by HMO granulation. In this research, macroporous $LMO/Al_2O_3(MLA)$ was created to reduce the performance barrier for Li adsorption as in Figure 17. Mesopores abound in cylindrical LMO/Al_2O_3 because to the highly porous-Al_2O_3.
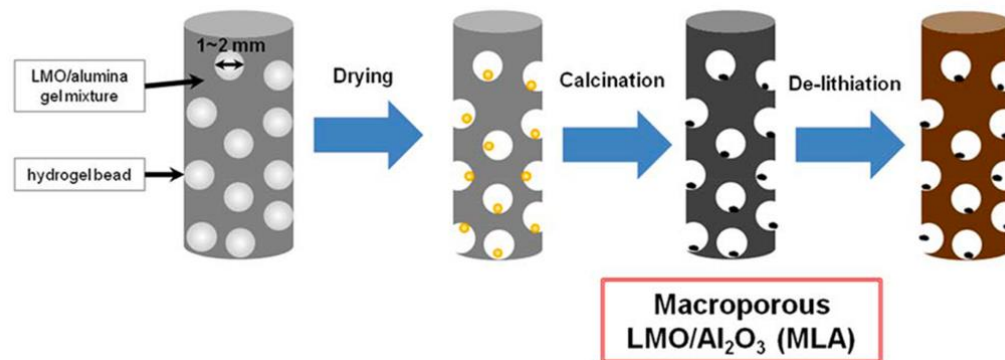
Figure 17. Macroporous LMO/Al$_2$O$_3$(MLA) Synthesis Procedure

Additionally, the inclusion of hydrogel beads induces the formation of macropores in LMO/Al$_2$O$_3$. The hydrogel beads broke down during calcination, leaving spherical macropores (500–1000 m). Li adsorption efficiency of MLAs was assessed in seawater that had been spiked with Li after delithiation. All MLAs showed equal Li adsorption capabilities at high Li concentrations. However, only MLA with the highest macropore density (porosity 60.3%) demonstrated Li uptakes comparable to those of HMO powder at low Li concentrations (50 mg/L). The driving force for Li adsorption was weak in a diluted Li solution, like seawater, and Li preferred to react with the HMO in macropores over that of mesopores (H. J. Hong et al. 2019)

In the work of Zandvakili and Ranjbar, in order to extract lithium from natural brine, a new ion exchange composite made of poly vinylidene fluoride (PVDF) is described in this work along with its characteristics and use. As an inorganic ion-exchange adsorbent, synthesized MnO$_2$ nanoparticles (HMO, final MnO$_2$ ion-sieve) that had good selectivity towards lithium adsorption were employed. The final MnO$_2$ ion exchange composite (CHMO) was created by first dissolving PVDF in N-methyl-2-pyrrolidone and then combining it with (HMO) in equal parts.
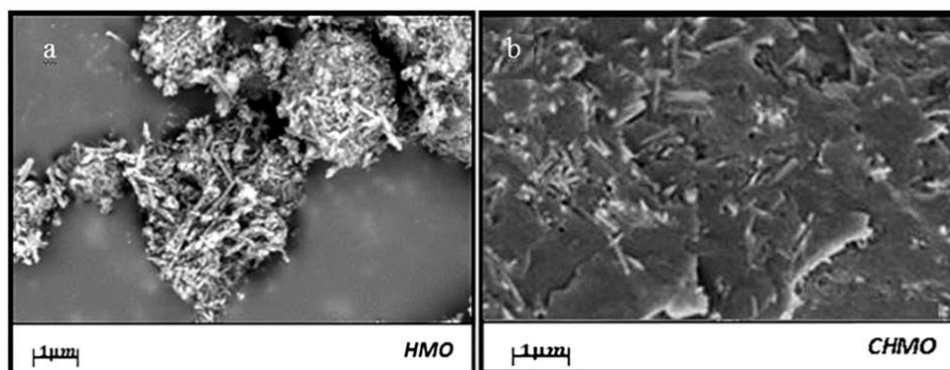
Figure 18. SEM images of HMO and CHMO

After drying at 220°C, the created solution serves as a binder and also a support to tightly connect HMO into a uniform 3-D interconnected network can be seen from Figure 18. The mesoporous/macroporous nature of this composite allows for the unrestricted flow of the solution. In lithium solution and the lithium-rich Lake Urmia, it demonstrated impressive Li adsorption capabilities of 19.22 and 11.06 mg (Li^+) g^{-1} (CHMO), respectively. Improvements to CHMO's overall performance are continuously being worked on (Zandvakili and Ranjbar, 2018)

In the study of Lin et al. with hydrothermal treatment of the core-shell structured C@TiO_2 using a EtOH/H_2O solution of LiOH and then calcining it in N_2 media, yolk-shell structured C@$Li_4Ti_5O_{12}$ microspheres with a carbon core (about 500 nm) and sea urchin-like $Li_4Ti_5O_{12}$ shell (approximately 400–500 nm) are created. Through acid treatment, C@$Li_4Ti_5O_{12}$ is further converted into a yoke-shell structured TiO_2-type lithium-ion sieve with a high specific surface area of 201.74 m^2/g. The composite exhibits a Li^+ adsorption capacity proportional to a pH value between 7 and 13. The ion exchange
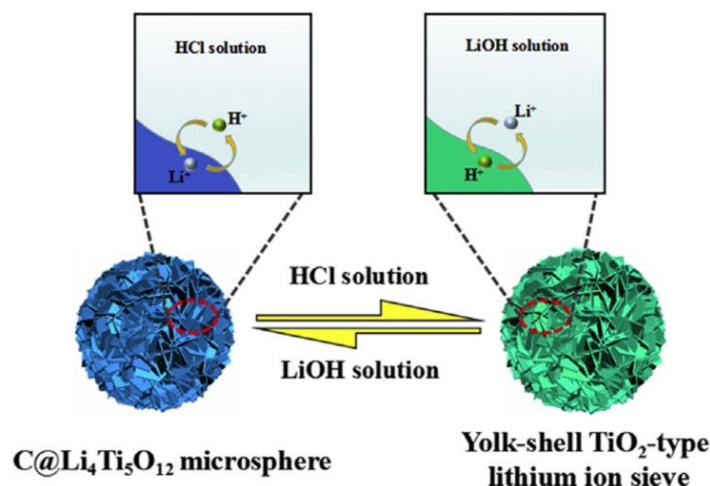
Figure 19. Illustration of the Li$^+$ and H$^-$ exchange on the spheres

The improved adsorption is attributed to the created accessible surficial voids by replacing the internal part with light carbon core, as evidenced by the fact that the adsorption reached equilibrium in 2 hours of time with a greater equilibrium adsorption capacity of 28.46 mg/g in alkaline conditions, which was nearly 8 times the value of ordinary TiO$_2$ lithium-ion sieve with similar size and surface area. The high-rate constant of 0.015 g/(mg·min). Adsorption reflects Freundlich and pseudo-second-order kinetic models and the ion exchange can be seen from Figure 19. The selective adsorption to Li$^+$ is confirmed when K$^+$, Na$^+$, Ca^{2+} and Mg^{2+} are present (Li et al. 2018).

In the study of Lawagon et al., systematically evaluating various polymers as matrix for H$_2$TiO$_3$ Li$^+$ adsorbent. For Li$^+$ adsorption tests, H$_2$TiO$_3$/polymers were electro spun as nanofibers (NF), described, and assessed using RSM with a central composite design. The best H$_2$TiO$_3$ support was found to be polyacrylonitrile (PAN) as shown in Figure 20. The hydrophilicity of H$_2$TiO$_3$/PAN and its advantageous NF structure allowed enough feed interaction. With a maximal capacity of 72.75 mg g^{-1} and an adsorption rate of 1.89×10^{-4} g mg^{-1} min^{-1}, the Li$^+$ adsorption was of the Langmuir type.
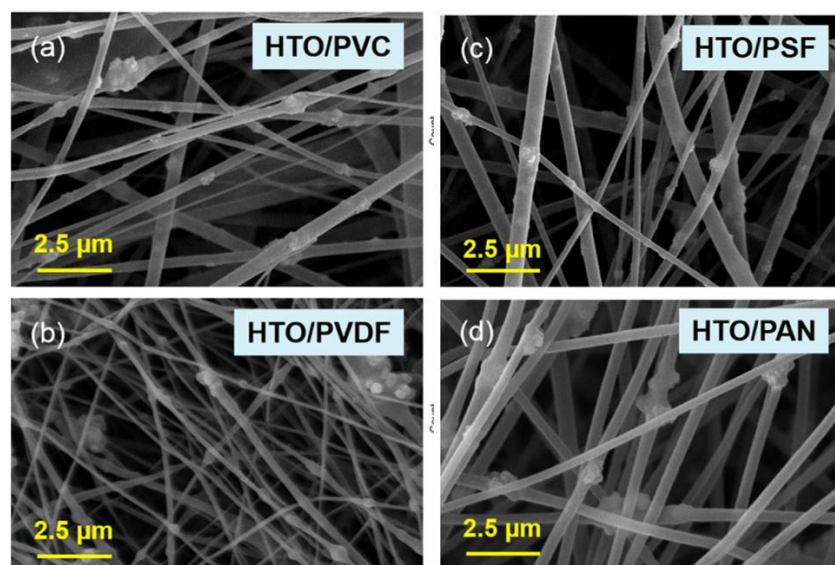
Figure 20. FE-SEM images (a–d) of HTO/Polymer NIFs

Li^+-selective H_2TiO_3/PAN has a thermodynamically advantageous adsorption. H_2TiO_3/PAN NF is a highly efficient composite Li^+ adsorbent, as demonstrated by its consistent performance and durability during cycled adsorption/desorption runs (Lawagon et al. 2019).

From the study of Limjuco et al., a good candidate lithium-ion sieve (LIS) that can replace the conventional manganese oxide-based LIS is metatitanic acid (H_2TiO_3). The H_2TiO_3 (HTO) was transformed into pliable composite foams in order to actualize its potential usage in continuous Li^+ recovery. Pre-synthesized HTO particles were mixed, lyophilized, and chemically cross-linked into a poly (vinyl alcohol) (PVA) matrix to create HTO/PVA and the SEM image was shown in Figure 21. With this strategy, the high quality and simple loading management of HTO in the foam were guaranteed. The composites' Li^+ adsorption capacity and mechanical toughness were thoroughly investigated and assessed. In comparison to the evenly dispersed unsupported HTO powder, the HTO/PVA had a low-capacity loss of 6% and a low retardation in Li^+ absorption rate of 8% at 200 wt% HTO loading. The large open pore network, consistent HTO distribution, and outstanding wettability of the foam are responsible for this superior performance.
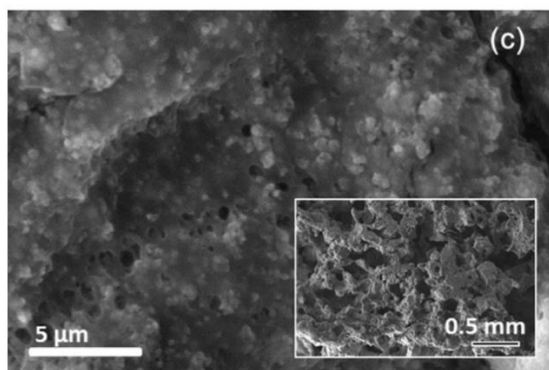
Figure 21. SEM image of HTO/PVA foam

The composite also kept hydrogen titanium oxides' Li$^+$ selectivity in seawater, indicating that there was almost no metal ion adsorption on the support matrix. The foam's great adaptability for long-term application in Li$^+$ mining from liquid resources like saltwater was demonstrated by the fact that it kept its performance and mechanical stability after multiple usage (Limjuco et al. 2016).

In this work of Lin et al., a unique composite lithium ion-sieve was created and used to recover lithium from geothermal water. By granulating the material using acid-alkali resistant polyvinyl chloride as a binder, the stability of the material was successfully solved. Additionally, the adsorption capabilities of the material were improved by employing polyethylene glycol as a porogen to create a porous structure and the synthesis was shown in Figure 22.

Figure 22. PVC-HTO synthesis

The created material has an adsorption capacity of 12.84 mg/g at the temperature of 328.15 K and an equilibrium period of roughly 12 h when it was used to remove lithium from geothermal water. To achieve cycle use, the material can be effectively regenerate using 0.25 mol/L HCl. The depreciation of adsorption capacity after five cycles was no more than 2%, and the separation factors for Li+ and other co-existing

ions separation were in found between 273.58–521.28. The polyporous ion-sieve is a possible contender for the lithium recovery from geothermal water selectively at low concentrations and proved to be reusable (Lin et al. 2019).

From the work of Chen et al., it is still extremely difficult to enhance the post-separation performance of powdered LIS while ensuring high adsorption capacity and quick kinetics. Here, an innovative, and porous titanium-based lithium-ion sieve (PIS) granules was created with the help of agar and is being utilized to collect lithium from geothermal water. The agar served as a sacrificial shaping element which is also porogenic agent and the sphericity of the PIS was shown in Figure 23. Since powdered ion sieve (IS) can be easily separated with filtration and then reused again with a consistent performance.
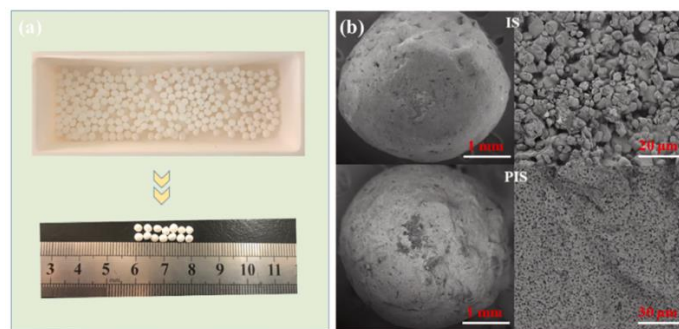
Figure 23. PIS and IS spheres' digital photos (a) and SEM images (b)

PIS had 64 times bigger diameter (2.8 mm) than IS. PIS demonstrated significant adsorption capacity of 25.8 mg/g, and quick kinetics (equilibrium was reached in 6 hours) in geothermal water due to its loose microstructures and abundant porosity. Additionally, in naturally occurring geothermal water, the separation factors of competitive ions associated to Li^+ were 1162.3, 273.7, and 328.5 for Na^+, K^+, and Ca^{2+}, respectively. Because of its improved post-separation capability, high capacity, and quick kinetics, this granular PIS can be an effective material for recovering lithium from geothermal water. Additionally, other porous adsorbents might be easily prepared using this straightforward and environmentally friendly process (Chen et al. 2021).

The summary of the literature survey including the Li^+ concentration, adsorption capacity and equilibrium time were given in Table 2.

Table 2. Mn based adsorbents in the literature and their comparison

Adsorbent	Sample	Li$^+$ Concentration (mg/L)	Adsorption Capacity (mg/g)	Equilibrium Time (h)	Reference
LiMn$_2$O$_4$ foams	LiOH solution	2395	20.9	24	(Han, Kim, and Park 2012)
LiMnO$_2$/PVA	LiOH solution	7	6.9	24	(Nisola et al. 2015)
H$_{1.6}$Mn$_{1.6}$O$_4$/PAN	LiCl/LiOH solution	35	10.3	24	(Park et al. 2014)
HMO/Al$_2$O$_3$	Seawater	29.8	6.2	72	(H.-J. Hong et al. 2018)
HMO/AAB	Seawater	28.5	8.87	144	(H.-J. Hong et al. 2015)
HMO/AL	LiCl solution	29.35	24	48	(Koilraj et al. 2016)
Chitosan/HMO	Seawater	30	11.4	168	(Moazeni et al. 2015)
HMO/Al$_2$O$_3$	Seawater	30	15	499	(H. J. Hong et al. 2019)
HMO/PVDF	LiOH solution	117.98	19.22	120	(Zandvakili and Ranjbar 2018)
C@Li$_4$Ti$_5$O$_{12}$	LiOH solution	1197.5	28.46	2	(Li et al. 2018)
HTO/PAN	Li$^+$ solution	70	32	24	(Lawagon et al. 2019)
PVA/HTO	LiCl/LiOH solution	7	12	12	(Limjuco et al. 2016)
PVC-HTO	Geothermal water	25.78	11.35	12	(Lin et al. 2019)
PIS-4	Li$^+$ solution	-	34.23	4	(Chen et al. 2021)
PIS-4	Geothermal water	25.8	12.29	6	(Chen et al. 2021)

CHAPTER 4

MATERIALS AND METHODS

4.1. Materials

The chemicals that were used in this study were given in the Table 3 below.

Table 3. Chemical used in the Synthesis of the Adsorbent

Chemicals	Chemical Formula	Manufacturer
Manganese (II) nitrate hexahydrate, 98%	$H_{12}MnN_2O_{12} . 6H_2O$	ABCR
Epichlorohydrin, 99%	C_3H_5ClO	Alfa Aesar
Sodium Hydroxide (Extra Pure)	NaOH	Tekkim Kimya
Potassium Hydroxide	KOH	Merck
Chitosan		Aldrich
Lithium Hydroxide monohydrate, 99.5%	$HLiO . H_2O$	Fisher
Hydrochloric Acid	HCl	Tekkim Kimya
Sodium Chloride	NaCl	Merck
Ammonium peroxodisulfide	$(NH_4)_2S_2O_8$	Merck

4.2. Adsorbent Synthesis

4.2.1. Synthesis of $Li_{1.6}Mn_{1.6}O_4$ (LMO)

In order to produce 100 mL of 1.0 mol/L $Mn(NO_3)_2$ solution, 28.7 g of $Mn(NO_3)_2$ $\cdot$ $6H_2O$ was dissolved in deionized water. 100 mL of 0.5 mol/ L $(NH_4)_2S_2O_8$ solution was prepared by solving 11.4 g of $(NH_4)_2S_2O_8$ in deionized water. 8.4 g of $LiOH \cdot H_2O$ was used to prepare 100 mL of 2.0 mol/L LiOH. Then, the prepared LiOH solution was put into an Erlenmeyer flask dropwise, into the $Mn(NO_3)_2$ solution under vigorous stirring. After the LiOH solution was added, 42.0 g of powdery $LiOH \cdot H_2O$ was put into the solution and stirred until a white precipitate was formed. The resulting solution was held in air at room temperature for 2 hours. Then, the resulting solution was brought up to 80°C, and the prepared solution of $(NH_4)_2S_2O_8$ was introduced dropwise with gentle stirring for 10 hours. The precipitate turned black, and was filtered, washed with deionized water until the conductivity of deionized water was reached for filtrate. Resulting adsorbent was dried under vacuum at 120°C for 12 h. The precipitate $Li_{1.6}Mn_{1.6}O_4$ (namely Li-type adsorbent, LMO) was sintered at 600°C for 24 h in an electricity heated oven. The experimental procedure shown below in Figure 24
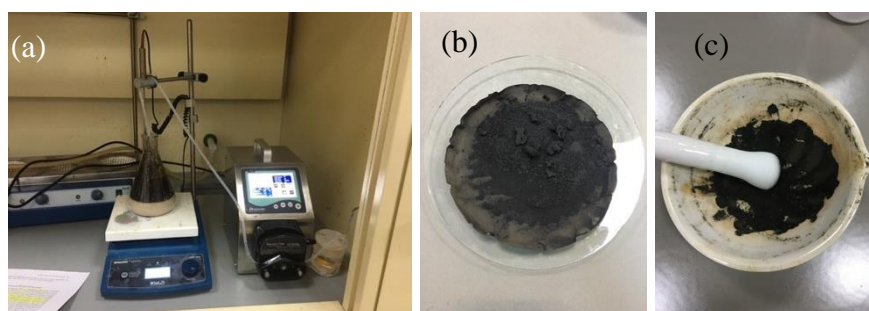
Figure 24. (a) Experimental setup of $Li_{1.6}Mn_{1.6}O_4$ synthesis (b) LMO before grinding and (c) grinded LMO

4.2.2. Preparation of Spherical Chitosan/λ MnO_2 adsorbent (CTS/LMO)

To granulate the adsorbent, a solution of 3.00 g of chitosan and 97 mL of 2% glacial acetic acid was prepared at room temperature. After the solution was homogenous, 2.00 g of LMO was introduced to the solution and mixed until a

homogenous black mixture was achieved. Then, the chitosan-LMO mixture was extruded into 1 mol/L NaOH solution to form spherical CTS/LMO granules. These spheres were washed with deionized water until the pH 7 was reached. After that CTS/LMO composites were dried for 12 hours at 60 °C. The experimental procedure shown below in Figure 25
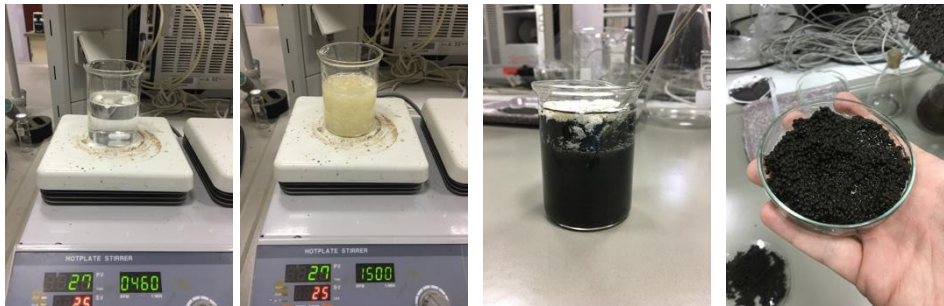
Figure 25. Procedure of Preparation of Spherical Chitosan/λ MnO2 adsorbent (CTS-LMO)

A chemical process called cross-linking causes the monomers to combine and create a structure that resembles a net. Better mechanical and chemical qualities than before can be found in cross-linked polymers. Numerous experiments have already been done to cross-link chitosan to enhance its chemical characteristics. There are numerous cross-linking agents for chitosan (H. J. Hong et al. 2013).
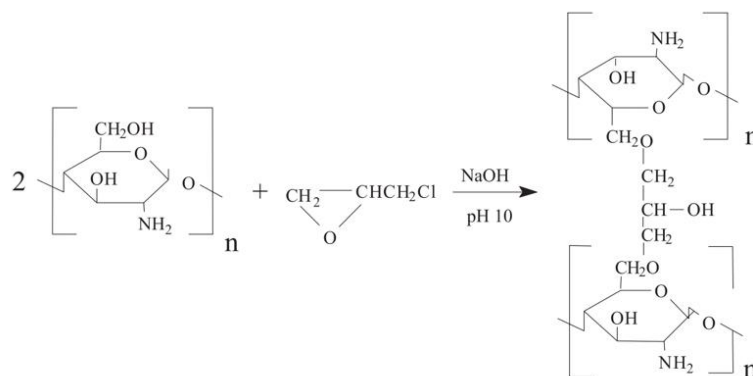
Figure 26. Crosslinking procedure of chitosan treated with epichlorohydrin

The granules' mechanical stability was improved by cross-linking as well. In general, when the starting concentration of Li^+ is high and the pH is alkaline, hydrogen manganese oxide (HMO) shows better Li^+ adsorption capacity. All the HMO powders in granules can reach the water completely because chitosan is a hydrophilic and water-permeable polymer.

4.2.3. Crosslinking of CTS/LMO with Epichlorohydrin

Epichlorohydrin, often known as ECH, is an epoxide and an organochlorine substance. It is a colorless liquid with a strong, garlic-like odor that is miscible with the majority of polar organic solvents but only mildly soluble in water. The experimental procedure shown below in Figure 27.
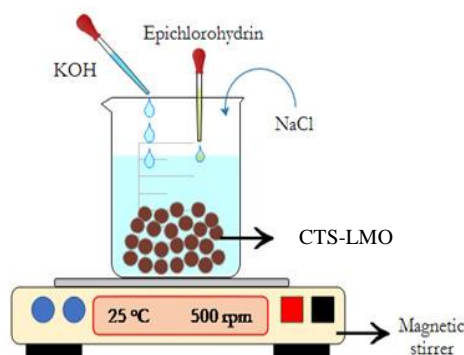
Figure 27. Procedure of Crosslinking of CTS/LMO with Epichlorohydrin

In a glass beaker, 5 grams of CTS/LMO, 0,075 grams of sodium chloride and 75 ml of water solution that had 0.35 ml of epichlorohydrin mixed to make a slurry. After that 0.3 grams of potassium hydroxide which was dissolved in 2 mL pure water was slowly added to the mixture for 15 minutes. Then the slurry was mixed for 16 hours at 25 °C. After that, the remaining was filtered and the filtrate was dried at 70 °C for overnight.

4.2.4. Delithiating the CTS/LMO to CTS/HMO

To obtain lithium from the aqueous media, spherical CTS/LMO must be transformed to CTS/HMO form to make it selective towards lithium. To obtain this crosslinked material (CTS/HMO), CTS/LMO was shaken in 0.25 mol/L, 500 mL HCl solution for 12 hours. After the procedure, the mixture was filtered and washed with deionized water till the pH around 4-5 was achieved. Then the CTS/HMO was dried at 60 °C for 12 hours.

To sum up the adsorbent synthesis, the change in the physical appearance on different stages can be seen in Figure 28 below. The color of the adsorbent changed to slightly dark red because of the content of manganese on the adsorbent.
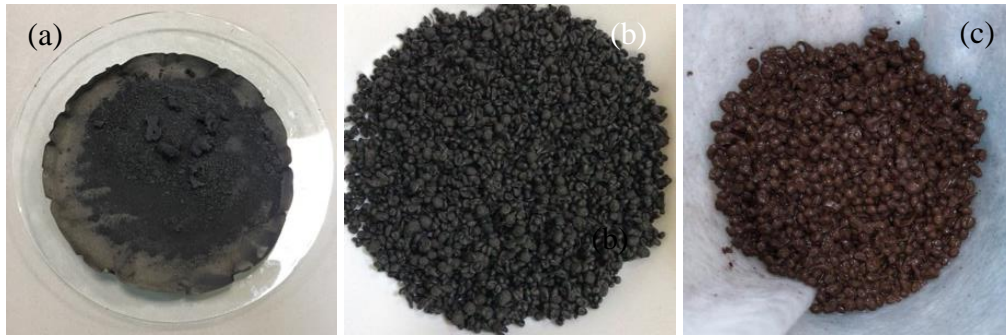
Figure 28. Three forms of adsorbent which are (a) before binding with chitosan
(LMO), (b) after binding with chitosan and crosslinked with epichlorohydrin
(CTS/LMO) and (c) delithiating with HCl which is the final product
(CTS/HMO).

4.3. Adsorption Studies

The adsorption studies were performed as batch experiments, using a stock solution of lithium chloride. The experiments were performed at water bath incubator for 24 hours. To determine the optimum adsorbent amount, adsorbent dosage effect was investigated using various adsorbent masses. For investigating the pH effect CTS/HMO was equilibrated while the pH ranged from 2 to 12. The effect of initial concentration and temperature investigated using Li solutions with concentrations of 10, 25, 50, 75, and 100 mg/L and at temperatures of 25, 35 and 45 °C.

To determine the kinetic characteristics of CTS/HMO, Li adsorption kinetic tests were performed. The interaction between the lithium ions adsorbed on the synthetic adsorbent was investigated using the two widely used Langmuir and Freundlich isotherm models with the experimental data. Also, thermodynamics of the adsorption was investigated in order to determine the thermodynamic parameters of the adsorption process. Desorption studies performed at various concentrations of HCl solution to desorb/extract Li from CTS/HMO to understand the desorption behavior of the CTS/HMO adsorbent on the reusability and Li recovery.

$$R\% = \frac{(C_i - C_e) \times 100}{C_i} \qquad\qquad Eq.\ 2$$

$$q_e = \frac{(C_i - C_e) \times V}{M_{(ads)}} \qquad\qquad Eq.\ 3$$

Detailed experiment conditions were given in Chapter 5.2 for each experiment separately. These experiments were run with two parallels to reduce the experimental error. Analysis of the lithium concentration was performed with ICP- OES analysis. The lithium recovery percentage was calculated using *Eq. 2* and adsorption capacity was calculated by *Eq. 3*

CHAPTER 5

RESULTS AND DISCUSSION

The main objective of this study was to recover lithium ion from lithium rich water resources with lithium manganese oxide by adsorption. Description of the material synthesis was given in the previous chapter. Characterization of the materials using analytical techniques such as SEM-EDX, XRD and BET analysis were done in order to characterize the synthesized lithium manganese oxide. Adsorption studies along with kinetics and thermodynamic studies related to adsorption process were done. Adsorbent sustainability was investigated with desorption studies and were described in this chapter.

5.1. Characterization Studies

Characterization of the lithium manganese oxide samples and chitosan were carried out by Integrated Research Centre (IRC) in the Izmir Institute of Technology (IZTECH). The three forms of the adsorbent were shown in Figure 28

5.1.1. SEM-EDX Analysis

Scanning electron microscopy was used for visual inspection of the surface morphology of the samples. While operating the scanning electron microscope (Quanta 250 SEM) at an accelerating voltage range of 3.0-5.0 kV, thin films of gold (Emitech K550X) was applied to the materials' free surfaces and as a result the photomicrography was produced. Energy Dispersive Spectrometer (EDS) and SEM were used to determine the chemical compositions of unaltered and changed materials (Al-Absi, Abu-Dieyeh, and Al-Ghouti 2021). All samples were examined at a 1000X magnification. Elemental composition of the adsorbents was given in the Figure 29.
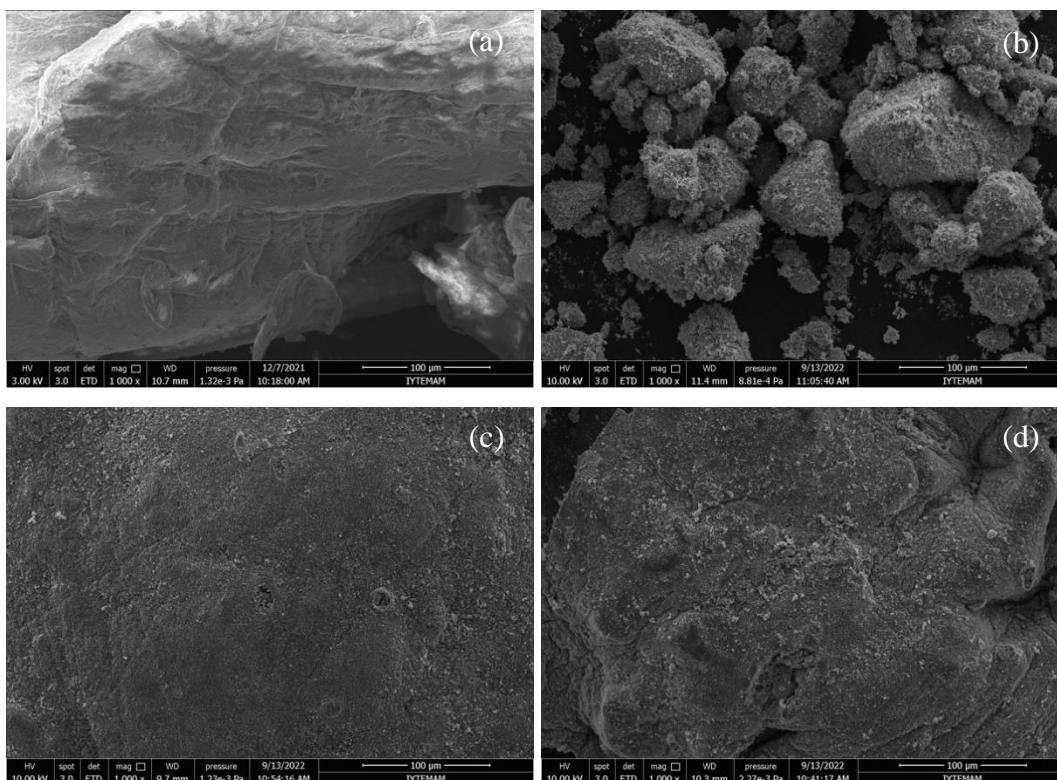
Figure 29. SEM micrographs of (a) chitosan, (b) lithium manganese oxide powder, (c) powder granulated with chitosan and crosslinked with epichlorohydrin, (d) adsorbent delithiated with 0.25M HCl at magnification 1000x

As shown in the Figure 29, the granulation of the powder (b) with chitosan (c) was made a polymer layer on the surface. The surface of CTS/LMO was smoother than LMO. Also, the adsorbent agglomerated together, and they become wider and bigger than manganese oxide powder. After the delithiation with 0.25M HCl, the surface become rough again but not as rough as the powder form (b). This phenomenon was attributed to the crosslinking the adsorbent with epichlorohydrin. According to the literature (Vanessa L. Gonçalves, n.d.) the roughness on the surface increases with the crosslinking agents. Also, the SEM images showed that, crosslinking the adsorbent with epichlorohydrin made the surface rougher with the polymer layer that was used.
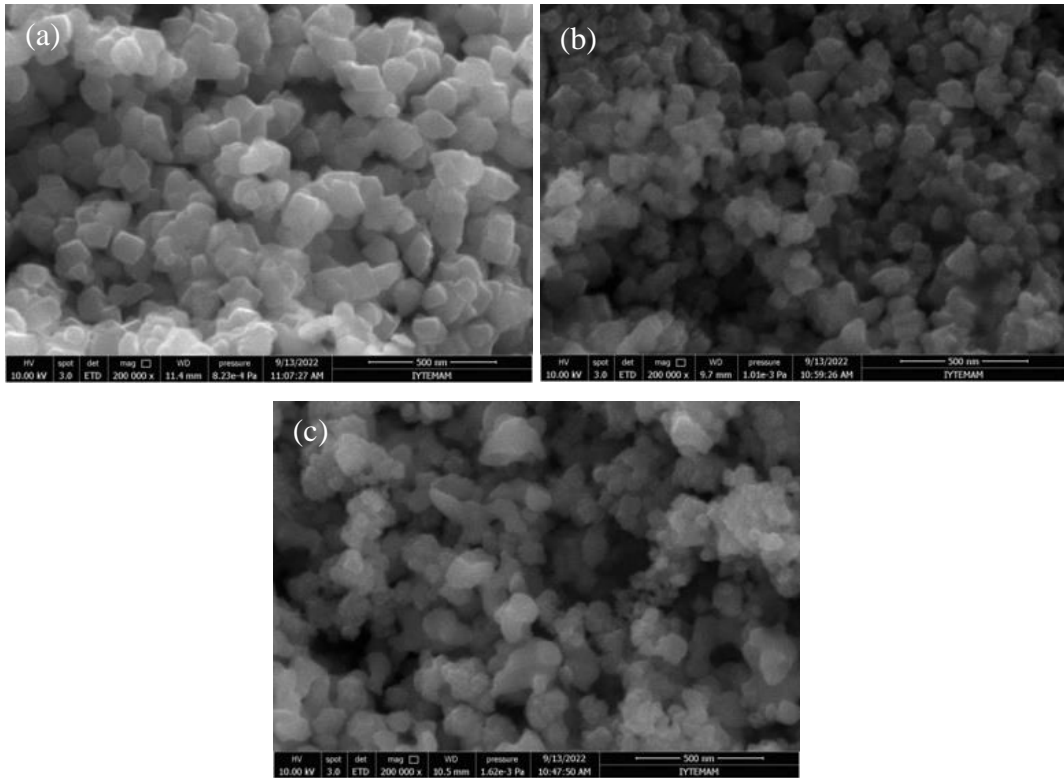
Figure 30. SEM Micrographs of (a) LMO powder, (b) CTS-LMO and (c) CTS-HMO
at 200000x magnification

The micrographs in Figure 30 shows the LMO powder, CTS-LMO and CTS-HMO. The surface morphologies were also similar to the synthesized nano lithium manganese oxide in the literature (Pulido et al. 2022). Also, the samples had mixed granular and cubic morphologies.

The elemental composition analysis showed additional presence of chloride in CTS-HMO due to crosslinking with epichlorohydrin. The tabulated composition data were given in Table 4. below and the energy dispersive spectra of the final product shown in Table 4 below.

Table 4. Elemental Compositions of Chitosan, LMO Powder, CTS-LMO and CTS-HMO in average atomic %

			Chitosan	LMO Powder	CTS-LMO	CTS-HMO
Element Average Atomic (%)	Carbon	(C)	46.14	2.22	20.43	31.22
	Oxygen	(O)	43.18	39.37	45.27	44.36
	Manganese	(Mn)	-	57.59	30.98	15.62
	Chloride	(Cl)	0.20	-	-	6.52
	Aluminum	(Al)	0.55	0.63	0.24	2.19
	Sodium	(Na)	0.14	-	-	0.07
	Nitrogen	(N)	9.57	-	2.58	-
	Cooper	(Cu)	0.21	-	-	-
	Potassium	(K)	-	-	0.09	-
	Calcium	(Ca)	-	-	0.08	-
	Zinc	(Zn)	-	-	0.33	-
	Silicon	(Si)	-	0.19	-	-
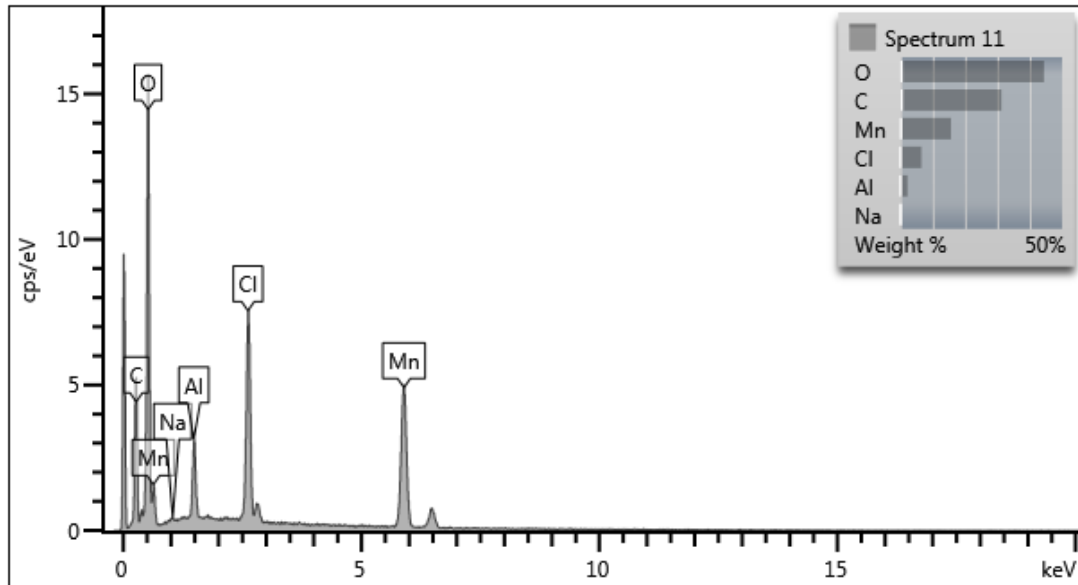
Figure 31. Energy Dispersive Spectra of CTS-HMO

The manganese amount in the final product (CTS/HMO) which was obtained from the EDX analysis, as shown in Figure 31 above, matches with the study of Park et al., (2014) but the amount of carbon and oxygen differs. This difference can be attributed to their polyacrylonitrile (PAN) usage instead of chitosan and epichlorohydrin (used in this study) in their study.

5.1.2. XRD Analysis

The crystalline phase structures were investigated using X-Ray Diffraction analysis (with a PhilipsX'PertPro device using Cu-Ka radiation as X-ray source, with a generator voltage of 45 Kv and tube current 40 mA, K-Alpha1 with 1.54056 wavelengths, K-alpha 2 with wavelength 1.54 at a ratio of K-Alpha2/K-Alpha1 as 0.5, with angle (θ–2θ), range of 80.00.
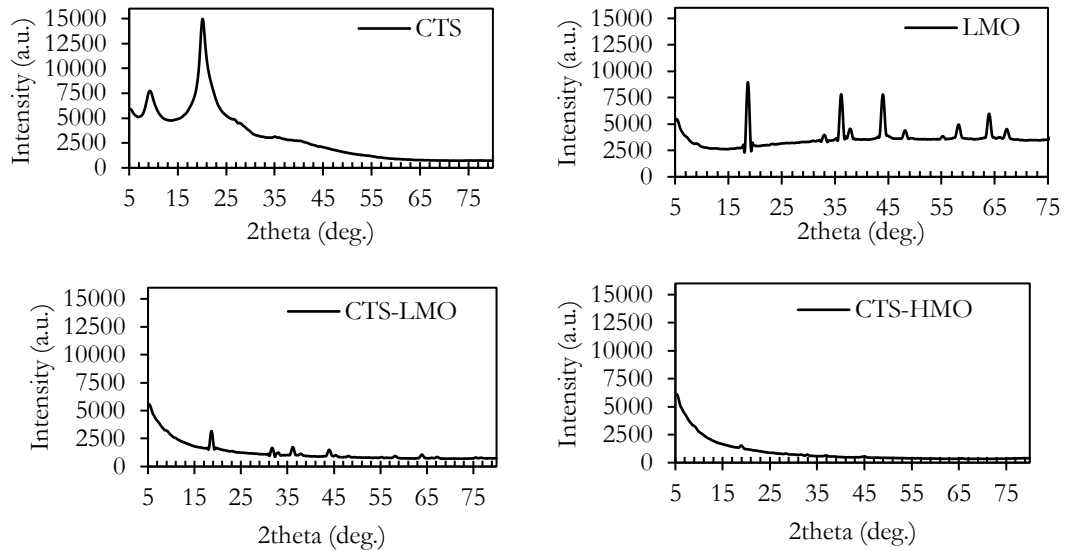
Figure 32. XRD Peaks of Lithium Manganese Oxide Adsorbent

From the XRD results (Figure 32), the crystallinity on the final product (CTS-HMO) were similar to the research reported by Zhang et al., (2021) and the addition of chitosan affected the crystal structure of the material. Also, the crosslinking with epichlorohydrin affected the crystalline structure as the crosslinking introduced amorphic nature. Also, the synthesized LMO showed almost identical XRD patter with the LMO synthesized by Roobavannan et al., (2020), indicating a successful LMO synthesis.
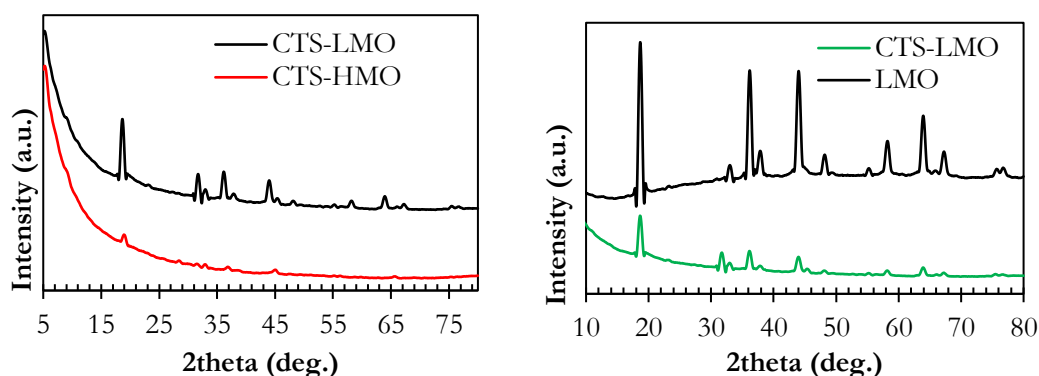
Figure 33. Comparison of Different XRD peaks

When we compare the peak at 20° for CTS-LMO and CTS-HMO from Figure 33, the peak become smaller in CTS-HMO with the treatment of HCl. The reason of this may be the delithiating of the adsorbent. With the addition of chitosan, there were no peaks added or removed to LMO, only the intensity of the peaks was decreased. Hence, the chitosan addition did not change the crystalline structure of the adsorbent significantly.

5.1.3. BET Surface Area

The pore size and pore size distributions were measured with BET surface area analysis (using a Micromeritics Gemini V, with Micromeritics VacPrep 061 Sample degassers, using N_2-adsorption). The pore sizes and surface area results were given in Table 5 below.

Table 5. BET surface area and pore size analysis of LMO Powder and CTS-HMO

Material	BET Surface Area (m^2/g)	Pore Size (nm)
LMO Powder	8.4091	7.3
CTS-HMO	0.1851	-

BET surface area of the final product (CTS-HMO) was 0.1851 m^2/g. Considering that LMO powder has a surface area of 8.4091 m^2/g, after granulation, surface area was significantly reduced. Also, the LMO powder surface area size was similar with the article by H. J. Hong et al., (2013), which the LMO surface area was

9.42 m^2/g. In addition to surface area, the size of the pores of powder was 7.3 nm and classified as mesoporous according to literature (Sing, 1985)

5.2. Adsorption Studies

The adsorption studies with CTS/HMO were performed as batch experiments, using a solution of LiCl with various concentration. For the effect of temperature, water bath incubator was used, and pH value of the solutions were adjusted using solutions of 0.1 M sodium hydroxide and 0.1 M hydrochloric acid. Analysis of the Li concentration was performed with ICP- OES analysis.

5.2.1. Effect of Adsorbent Dosage

Using a solution of 10 mg/L lithium chloride, the experiments were conducted at room temperature for 24 hours to determine the effectiveness and ideal dosage of lithium manganese oxide adsorbent. To determine the optimum adsorbent amount, various adsorbent masses, 0.5, 1, 2, 4, and 8 g/L, were used and to lower the error percentage, each experiment was repeated twice.

As adsorbent dose was increased, Li$^+$ removal efficiency gradually improved until the optimum adsorbent concentration of 4 g/L was reached. This dosage was likewise thought to be the limit since, as shown in Figure 34, increasing the dosage amount further had no additional impact on Li removal.
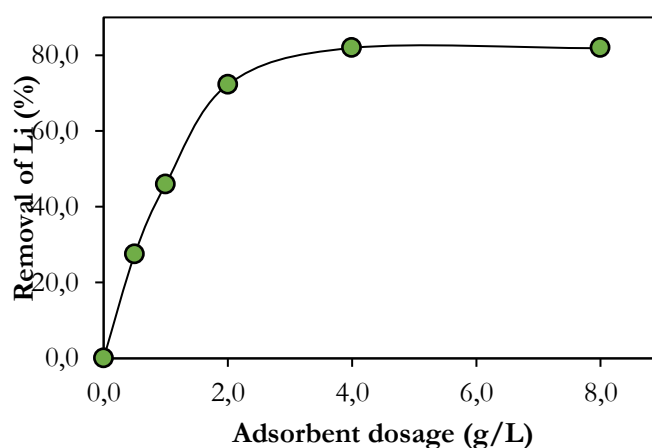
Figure 34. Adsorbent Dosage Effect

Increased CTS/HMO dosage resulted in more active sites being available on the adsorbent, which in turn increased Li ion recovery (S. Wang et al. 2018). When the

equilibrium between the quantity of adsorbent surfaces active sites and the quantity of lithium in solution was achieved, adsorbent saturation was reached. Since a further increase in adsorbent dosage did not increase the removal and would not be worth the production expenses, 4 g/L CTS/HMO dosage was chosen as the optimum dosage in all experiments.

5.2.2. Effect of pH

Effect of solution pH on adsorption process was investigated. 0.2g of LMO was equilibrated with 50 mL of 10 ppm LiCl solution in batch mode at 180 rpm, at room temperature while the pH ranged from 2 to 12. The desired pH values were adjusted using solutions of 0.1 M sodium hydroxide and 0.1 M hydrochloric acid solutions. The results of the pH experiment were given in Figure 35.
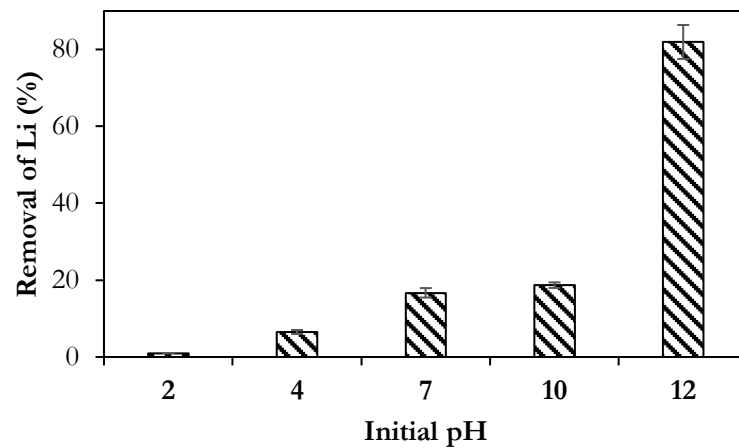
Figure 35. Effect of pH on the Removal of Li

From the Figure 35 above, increasing the -OH ions in the solution increased the adsorption performance as removal of Li was highest at pH 12. This situation can be explained by the performance increase of chitosan at basic conditions as explained by Lin et al., (2019). Also in the study of Qian et al., (2020) the performance of LMO type adsorbent increased as the pH rises, which may be explained by a shift in reaction equilibrium to the left, as pH rises in the Li+/H+ ion-exchange mechanism indicated in equation below:

$$H_{1.6}Mn_{1.6}O_4 + Li^+ \rightleftharpoons Li_{1.6}Mn_{1.6}O_4 + H^+$$
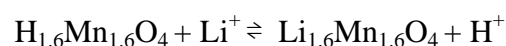
The point of zero charge of HMO was investigated at several pH ranges to better understand how pH and HMO interact with Li adsorption. The findings demonstrated that when pH increased, the point of zero charge for HMO got more negative and was calculated at 3.6 and tabulated in Figure 36.
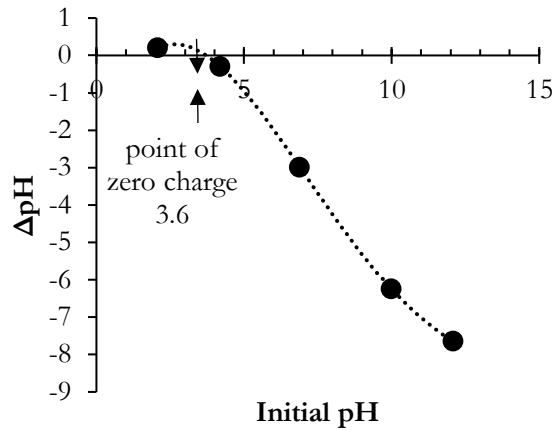
Figure 36. Point of Zero Charge

Positively charged ions are more effectively electrostatically attracted to an adsorbent (outer-sphere ion complexation) when its negative surface charge is increased. Therefore, it is probable that at higher pH levels, the increasing negative surface charge results in attraction of more positively charged Li ions (Roobavannan et al., 2020).

5.2.3. Effect of Initial Concentration and Temperature

In this section, the effects temperature and initial ion concentration on Li removal were examined. To comprehend the effect of temperature and initial concentration, Li solutions with concentrations of 10, 25, 50, 75, and 100 mg/L were contacted with 1 g of adsorbent for 24 hours at 180 rpm and pH 12. This study was conducted at 25 °C, 35 °C, and 45 °C with the suggested changing concentrations.
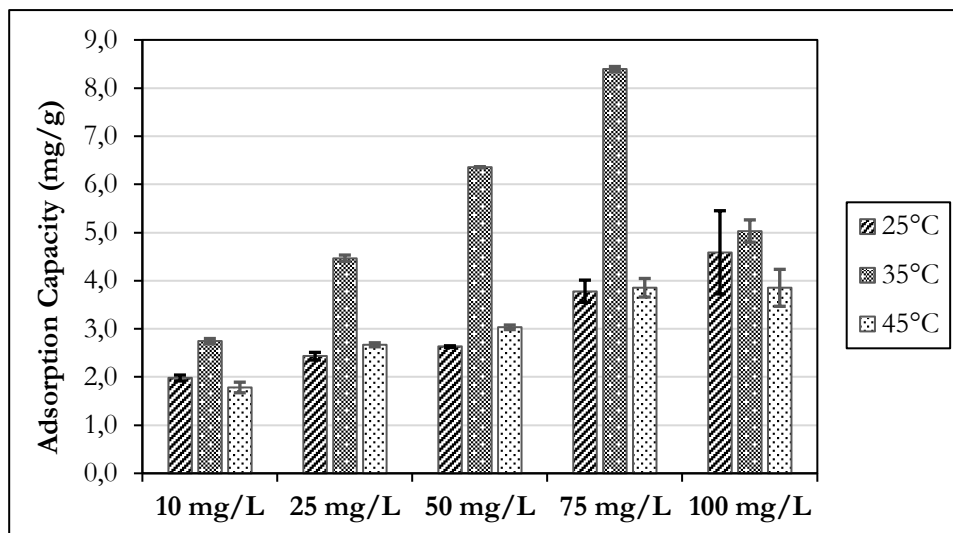
Figure 37. Adsorption Capacity of Various Initial Concentrations at Different
Temperatures

From Figure 37, the highest adsorption capacity was achieved at 35°C. This can be explained by the chitosan performance temperature. According to literature, raising the temperature might be able to enhance the CTS-HMO's ability to adsorb the metal ions (Zhang et al. 2021).

5.2.4. Adsorption Kinetics

To describe the adsorption mechanism and adsorption features, adsorption kinetics were studied. Contact time is a valuable data for the adsorbent capacity and adsorbent performance. Li adsorption kinetic tests were performed in 500 mL of LiCl solution at 30 °C and a pH of 12 with a rotational speed of 250 rpm. The experiment was repeated for three different LMO adsorbent concentrations, 1, 2, and 4 g/L. At intervals of 0, 5, 10, 15, 20, 30, 45, 60, 90, 120, 240, 360, 480, and 1440 minutes, samples were taken. After the samples were filtrated, the ICP-OES was used to determine the concentration of Li in the filtrate.

According to the contact time vs C/C_0 graph below in Figure 38, equilibrium was reached in approximately 9 hours with the adsorbent reaching the maximum adsorption capacity and the equilibrium time was similar even in various concentrations. Also, the concentration of Li^+ adsorbed on the adsorbent increases with the extended amount of time until the 500 minutes.
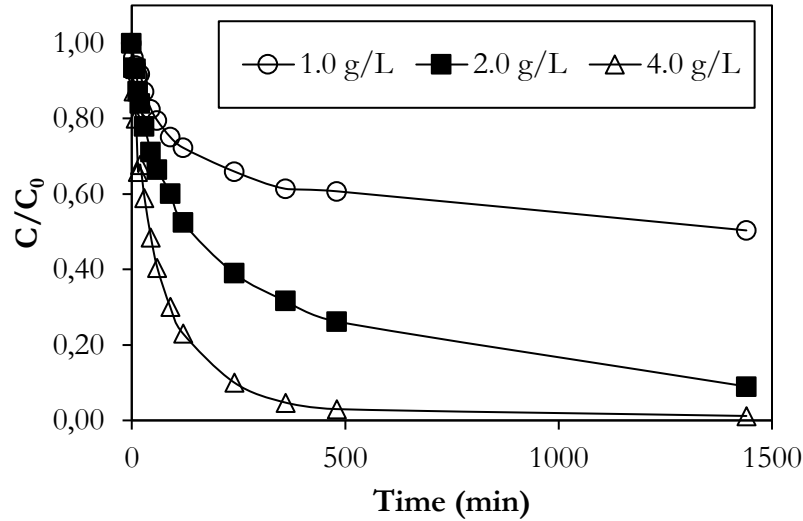
Figure 38. Adsorption Kinetics for Different Adsorbent Dosages

From the results, the adsorption of lithium on the CTS/HMO occurs quickly in one hour period. The kinetic behavior of the adsorbent was investigated using pseudo-first and pseudo-second order kinetic models and intraparticle diffusion models were applied to the experimental data. The kinetic models were given below:

The pseudo-first order kinetic model (Hameed, Tan, and Ahmad 2008) is defined in Eq. 4.

$$\ln(q_e - q_t) = \ln q_e - k_1 t \qquad\qquad Eq.\ 4$$

Where k_1 (min^{-1}) is the adsorption rate constant, and q_e and q_t (mg/g) are the amounts of adsorbate adsorbed at equilibrium and at any time, throughout the period of t(min).

Intraparticle diffusion model is an empirical relationship based on the theory of Weber and Morris and was given in Eq. 5.

$$q_t = k_i t^{1/2} + c_i \qquad\qquad Eq.\ 5$$

Where c_i is the adsorption capacity at equilibrium [mg.g^{-1}] and k_i is the intraparticle diffusion rate constant [mg.g^{-1}min$^{1/2}$]. C_i and k_i was calculated from intercept and slope of the plot of q_t versus $t^{1/2}$, respectively.

The linearized form of pseudo-second order equation based on equilibrium adsorption is shown in *Eq. 6*

$$\frac{t}{q_t} = \frac{1}{k_2 q_e^2} + \frac{1}{q_e} t$$
Eq. 6

Where q_e and k_2 are derived from the slope and intercept of the plot of t/q_t vs t, respectively, and k_2 (g/mg.min) is the rate constant of second-order adsorption.

From the Table 6 below, pseudo-first-order model gave the best fit with the R^2 value of 0.99 for all adsorbent dosages, therefore the adsorbent followed pseudo-first-order kinetics.

Table 6. Kinetic Comparison at Different Dosages

		1 g/L	2 g/L	4 g/L
Pseudo-first order kinetic	R^2	0.99	0.99	0.99
	q_e,theo (mg/g)	5.704	5.267	2.962
	k_1 (min^{-1})	0.008	0.0075	0.015
	q_e, calc (mg/g)	5.91	5.43	3.14
Pseudo-second order kinetic	R^2	0.97	0.93	0.99
	q_e,theo (mg/g)	4.269	3.619	2.939
	k_2 (g mg^{-1} min^{-1})	0.004	0.0054	0.0096
	q_e, calc (mg/g)	5.91	5.430	3.14
Intraparticle diffusion	R^2	0.98	0.97	0.98
	q_e,theo (mg/g)	2.175	2.272	2.191
	ki (g mg^{-1} min$^{-1/2}$)	0.097	0.096	0.098
	q_e, calc (mg/g)	5.905	5.430	3.141

5.2.5. Adsorption Isotherms

The adsorption behavior as the interactions between the lithium ions adsorbed on the synthetic adsorbent was investigated using the two widely used Langmuir isotherm and Freundlich isotherm models with the experimental data. While the Langmuir adsorption isotherm model defines the adsorption process with a single-layer homogeneous adsorption on the adsorbent surface, the Freundlich isotherm defines adsorption as multilayer, heterogeneous process presents on the surface (Altınbaş et al.

2022). The linearized forms of Langmuir model on the first equation and Freundlich model on the second were given as:

$$\frac{C_e}{Q_e} = \frac{1}{Q_m}C_e + \frac{1}{K_L Q_m} \qquad Eq.\ 7$$

$$\log Q_e = \frac{1}{n}\log C_e + \log K_F \qquad Eq.\ 8$$

Where q_e is the equilibrium adsorption capacity (mg/g), q_m (mg/g) is the maximum adsorption capacity found from the model and C_e (mg/L) is the equilibrium concentration of the adsorbate, K_L (L/mg) is the Langmuir constant K_F (L/g) and n are Freundlich adsorption constants. These isotherm calculations were done for three different temperature which are 25°C, 35°C and 45° and the model parameters were given in Table 7 and Table 8 below.

Table 7. Langmuir Isotherm Constants at Different Temperatures

Langmuir Isotherm	25°C	35°C	45°C
Q_{max}	4.9382	5.2882	4.1390
K_L	0.0606	-0.3499	0.1367
SSE	22.791	9.4117	1.0419
R^2	0.8885	0.9438	0.9894

Table 8. Freundlich Isotherm Constants at Different Temperatures

Freundlich Isotherm	25°C	35°C	45°C
K_F	1.3141	0.2315	1.3739
n_F	4.0600	1.5506	4.2390
SSE	0.081	13.8967	0.0112
R^2	0.8245	0.6945	0.9723

The correlation coefficients were given in Table 7. The Langmuir adsorption isotherm model showed the best fit to the experimental data with the correlation coefficient of (R_2 = 0.9894), which suggested that the adsorption process of Li^+ onto CTS/HMO followed the Langmuir model, indicating a single layer adsorption of lithium ions onto the surface of the adsorbent.

The maximum adsorption capacity, q_m was calculated from the model as 5.28 mg/g. When the capacity found from Langmuir model was compared with experimental adsorption capacity, there was no significant difference, which confirmed the goodness-of-fit of the model, thus, the adsorption capacity found from the Langmuir model was considered to be valid.

5.2.6. Desorption studies

In this analysis, various concentrations of HCl solution were utilized to desorb/extract Li from CTS/HMO. To desorb Li from CTS/HMO, HCl in concentrations of 0.25M, 0.5M, and 1.0M were used. 50 mL samples of 10 mg/L Li^+ solutions at pH 12 were used with 4g/L adsorbent dosage and two cycles of adsorption and desorption were applied. The results of adsorption and desorption experiments of two cycles were given in Figure 39 below.
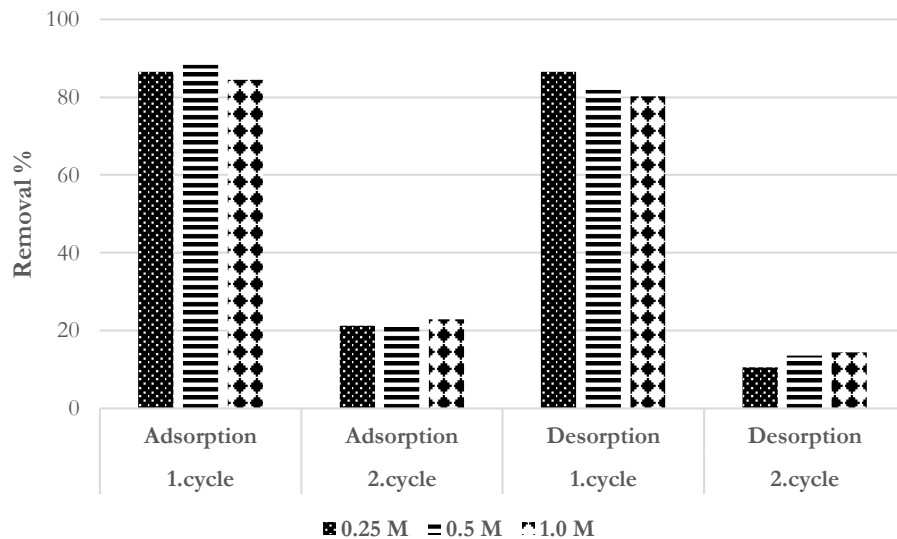
Figure 39. Lithium adsorption and desorption percentages

At the first cycle, 90% Li removal on average and close to 95% Li desorption was obtained with every HCl molarities. According to the results, 0.25 M HCl was chosen to extract Li from CTS/HMO and, for the regeneration of CTS/HMO since it gave the higher desorption percent (100%). With 0.25M HCl, desorbed Li amount was higher than adsorbed Li amount in the first cycle, which may have been caused by Li that was present in the first HMO and a similar result mentioned on the article of Roobavannan et al., (2020) in the literature. On the second cycle, there were remarkable

decreases (~80%) on adsorbed Li amounts and desorbed Li amounts (~50%) as seen in the Figure 39. This phenomenon was attributed to the structural deformity of the adsorbents after treated with HCl that was observed. The adsorbent size was reduced after the treatment and the grains were deformed, became more powdered than before. Since, the desorption using HCl was not suitable to reuse the adsorbent.

5.2.7. Thermodynamic studies

The optimal amount of adsorbent (4 g/L) at 25, 35, and 45° C was studied for lithium adsorption at varying concentrations (10 to 100 ppm) in order to estimate the thermodynamic parameters such as Gibbs free energy change (G°), enthalpy change (H°), and entropy change (S°). K_L values found from the Langmuir adsorption isotherm was employed to calculate the parameters from equations below:

$$\Delta G° = -RT \ln K_L \qquad\qquad Eq.\ 9$$

$$\ln K_L = \frac{\Delta S°}{R} - \frac{\Delta H°}{RT} \qquad\qquad Eq.\ 10$$

The slope (-3845.8) and intercept (18.308) of the $\ln K_L$ versus 1/T plot were calculated as shown in Figure 40 with the Van't Hoff equation, *Eq. 10* and the values for H and S were determined. Calculated thermodynamic parameters were tabulated in Table 9
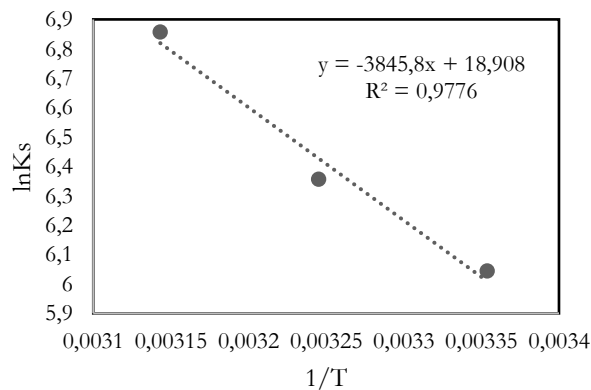
Figure 40. ln K_L versus 1/T plot

Table 9. Parameters of lithium adsorption thermodynamics onto CTS/HMO

T (K)	K_L	$\Delta G°$ (kJ/mol)	$\Delta H°$ (kJ/mol)	$\Delta S°$ (kJ/mol)
298.15	421	-14.89		
308.15	576.1	-16.46	31,97	0,15
318.15	949.5	-18.03		

Positive $\Delta H°$ suggests that lithium adsorption process was endothermic, while positive $\Delta S°$ was indicating that the randomness of the molecules at the adsorption surface increased. Also, $\Delta G°$ values for all temperature were negative and the reason of this was the spontaneous adsorption process. The found thermodynamic parameters were similar and all the found phenomena were same with the chitosan modified HMO based adsorbent in the literature (Zhang et al. 2021).

CHAPTER 6

CONCLUSION

The majority of investigations have surprisingly shown a lot of interest in batch adsorption studies. Although these new Li recovery techniques have yielded promising results, assuring their long-term viability and sustainability remains one of the primary challenges. A major challenge for all lithium recovery technologies has been figuring out what to do with the enormous amount of wasteful brine that remains after lithium recovery. Most of the published research has largely neglected this issue, and the conventional wisdom was to dispose of this brine in nearby salt lakes and underground aquifers. Conducting column-based research of adsorption systems would be more advantageous since the parameters discovered would be more valuable for comprehending the systems' potential for industrial application as well as for scale-up and costing considerations.

However, most advanced adsorbents are not commercially accessible and require a lot of time and energy to synthesize. Wide scale applications are not yet economically viable. Therefore, their synthesis is limited to minor amounts on a laboratory scale. In addition, the partial adsorption, and the presence of high concentrations of additional elements require more advanced adsorbents to achieve the required levels of purity. Even though adsorption-based systems are easier to construct, less expensive, and more effective for brines with low concentrations of lithium, the produced adsorbents have limited selectivity and poor regeneration.

This primary objective of this thesis was to produce an adsorbent which was selective to lithium ion, for the recovering lithium from water resources. The adsorbent was synthesized, granulated by chitosan afterwards the adsorbent crosslinked with epichlorohydrin to improve the adsorption efficiency. To verify the adsorbent's functionality SEM, EDX, BET surface area and XRD analysis were employed. From the characterization results the BET surface area calculated as 8.4091 m^2/g and the SEM and XRD results matches with the literature. Lithium manganese oxide adsorbent's crystallinity changes with the chitosan content and crosslinking with epichlorohydrin. In addition, the SEM micrographs proved that the adsorbent uniformly distributed.

The adsorption studies shows that the lithium manganese oxide adsorbent showed optimum removal performance at pH 12 and at 35°C. In addition, the ideal amount of adsorbent for lithium recovery from initial concentration of 10 mg/L was found as 4g/L with 91% removal efficiency. Currently, the best fit for the adsorption found as the Langmuir isotherm, which was showing a monolayer adsorption with a maximum capacity of q_m was found 5.2882 mg/g. The pseudo-first-order kinetic model also gave better explanation for the adsorption of lithium. Thermodynamically in all temperature ranges, adsorption was spontaneous and endothermic.

Finally, the study for desorption showed the lithium recovery was calculated as 100%, 92% and 94% for 0,25M, 0,50M and 1.0M HCl respectively which is a quite good recovery rate but at the second cycle adsorption and desorption rates were remarkably decreased, indicating that the HCl treatment was not a useful solution for reusability.

As the demand for portable electronics and electric vehicles grows exponentially, it is urgently necessary to focus on feasible lithium recovery from alternative sources to maintain supply and demand balance in the market going ahead.

Since most of the experiments done in batch adsorption test, recommendation oof column studies must be examined for further studies. Molecular modeling, economic analysis, and the disposal of spent adsorbents are needed to be done in the future studies.

REFERENCES

Al-Absi, Rana S., Mohammed Abu-Dieyeh, and Mohammad A. Al-Ghouti. 2021. "Brine Management Strategies, Technologies, and Recovery Using Adsorption Processes." *Environmental Technology and Innovation*. Elsevier B.V. https://doi.org/10.1016/j.eti.2021.101541.

Alessia, Amato, Becci Alessandro, Villen Guzman Maria, Vereda Alonso Carlos, and Beolchini Francesca. 2021. "Challenges for Sustainable Lithium Supply: A Critical Review." *Journal of Cleaner Production*. Elsevier Ltd. https://doi.org/10.1016/j.jclepro.2021.126954.

Altınbaş, Bekir Fırat, Ceren Orak, Hatice Eser Ökten, and Aslı Yüksel. 2022. "Novel Hybrid Adsorption-Electrodialysis (AdED) System for Removal of Boron from Geothermal Brine." *ACS Omega*, December. https://doi.org/10.1021/acsomega.2c06046.

Cetiner, Z S, Ö Doğan, G Özdilek, and P Ö Erdoğan. 2015. "Toward Utilising Geothermal Waters for Cleaner and Sustainable Production: Potential of Li Recovery from Geothermal Brines in Turkey Özgür Doğan Pembe Özer Erdoğan 'Toward Utilising Geothermal Waters for Cleaner and Sustainable Production: Potential of Li Recovery from Geothermal Brines in Turkey.'" *Int. J. Global Warming*. Vol. 7.

Chen, Shangqing, Zishen Chen, Zhenwei Wei, Jiayin Hu, Yafei Guo, and Tianlong Deng. 2021. "Titanium-Based Ion Sieve with Enhanced Post-Separation Ability for High Performance Lithium Recovery from Geothermal Water." *Chemical Engineering Journal* 410 (April). https://doi.org/10.1016/j.cej.2020.128320.

Hameed, B. H., I. A.W. Tan, and A. L. Ahmad. 2008. "Adsorption Isotherm, Kinetic Modeling and Mechanism of 2,4,6-Trichlorophenol on Coconut Husk-Based Activated Carbon." *Chemical Engineering Journal* 144 (2): 235–44. https://doi.org/10.1016/j.cej.2008.01.028.

Han, Yosep, Hyunjung Kim, and Jaikoo Park. 2012. "Millimeter-Sized Spherical Ion-Sieve Foams with Hierarchical Pore Structure for Recovery of Lithium from

Seawater." *Chemical Engineering Journal* 210 (November): 482–89.
https://doi.org/10.1016/j.cej.2012.09.019.

Hong, Hye Jin, In Su Park, Taegong Ryu, Byoung Gyu Kim, and Kang Sup Chung.
2019. "Macroporous Hydrogen Manganese Oxide/Al2O3 for Effective Lithium
Recovery from Seawater: Effects of the Macropores vs Mesopores." *Industrial
and Engineering Chemistry Research* 58 (19): 8342–48.
https://doi.org/10.1021/acs.iecr.9b01613.

Hong, Hye Jin, In Su Park, Taegong Ryu, Jungho Ryu, Byoung Gyu Kim, and Kang
Sup Chung. 2013. "Granulation of Li1.33Mn1.67O4 (LMO) through the Use of
Cross-Linked Chitosan for the Effective Recovery of Li+ from Seawater."
Chemical Engineering Journal 234 (December): 16–22.
https://doi.org/10.1016/j.cej.2013.08.060.

Hong, Hye-Jin, In-Su Park, Jungho Ryu, Taegong Ryu, Byoung-Gyu Kim, and Kang-
Sup Chung. 2015. "Immobilization of Hydrogen Manganese Oxide (HMO) on
Alpha-Alumina Bead (AAB) to Effective Recovery of Li+ from Seawater."
Chemical Engineering Journal 271 (July): 71–78.
https://doi.org/10.1016/j.cej.2015.02.023.

Hong, Hye-Jin, Taegong Ryu, In-Su Park, Mikyung Kim, Junho Shin, Byoung-Gyu
Kim, and Kang-Sup Chung. 2018. "Highly Porous and Surface-Expanded Spinel
Hydrogen Manganese Oxide (HMO)/Al2O3 Composite for Effective Lithium
(Li) Recovery from Seawater." *Chemical Engineering Journal* 337 (April): 455–
61. https://doi.org/10.1016/j.cej.2017.12.130.

Ighalo, Joshua O., James F. Amaku, Chijioke Olisah, Adedapo O. Adeola, Kingsley O.
Iwuozor, Kovo G. Akpomie, Jeanet Conradie, Kayode A. Adegoke, and Kabir O.
Oyedotun. 2022. "Utilisation of Adsorption as a Resource Recovery Technique
for Lithium in Geothermal Water." *Journal of Molecular Liquids*. Elsevier B.V.
https://doi.org/10.1016/j.molliq.2022.120107.

Khalil, Abdullah, Shabin Mohammed, Raed Hashaikeh, and Nidal Hilal. 2022.
"Lithium Recovery from Brine: Recent Developments and Challenges."
Desalination. Elsevier B.V. https://doi.org/10.1016/j.desal.2022.115611.

Koilraj, Paulmanickam, Siwaporn Meejoo Smith, Qianqian Yu, Sarah Ulrich, and Keiko Sasaki. 2016. "Encapsulation of a Powdery Spinel-Type Li+ Ion Sieve Derived from Biogenic Manganese Oxide in Alginate Beads." *Powder Technology* 301 (November): 1201–7. https://doi.org/10.1016/j.powtec.2016.08.009.

Lawagon, Chosel P., Grace M. Nisola, Rosemarie Ann I. Cuevas, Hern Kim, Seong Poong Lee, and Wook Jin Chung. 2019. "Development of High Capacity Li+ Adsorbents from H2TiO3/Polymer Nanofiber Composites: Systematic Polymer Screening, Characterization and Evaluation." *Journal of Industrial and Engineering Chemistry* 70 (February): 124–35. https://doi.org/10.1016/j.jiec.2018.10.003.

Li, Na, Deli Lu, Jinlong Zhang, and Lingzhi Wang. 2018. "Yolk-Shell Structured Composite for Fast and Selective Lithium Ion Sieving." *Journal of Colloid and Interface Science* 520 (June): 33–40. https://doi.org/10.1016/j.jcis.2018.02.031.

Limjuco, Lawrence A., Grace M. Nisola, Chosel P. Lawagon, Seong Poong Lee, Jeong Gil Seo, Hern Kim, and Wook Jin Chung. 2016. "H2TiO3 Composite Adsorbent Foam for Efficient and Continuous Recovery of Li+ from Liquid Resources." *Colloids and Surfaces A: Physicochemical and Engineering Aspects* 504 (September): 267–79. https://doi.org/10.1016/j.colsurfa.2016.05.072.

Lin, Hongyu, Xiaoping Yu, Mingli Li, Ji Duo, Yafei Guo, and Tianlong Deng. 2019. "Synthesis of Polyporous Ion-Sieve and Its Application for Selective Recovery of Lithium from Geothermal Water." *ACS Applied Materials and Interfaces* 11 (29): 26364–72. https://doi.org/10.1021/acsami.9b07401.

Moazeni, Maryam, Hengameh Hajipour, Masoud Askari, and Mohammad Nusheh. 2015. "Hydrothermal Synthesis and Characterization of Titanium Dioxide Nanotubes as Novel Lithium Adsorbents." *Materials Research Bulletin* 61: 70–75. https://doi.org/10.1016/j.materresbull.2014.09.069.

Nisola, Grace M., Lawrence A. Limjuco, Eleazer L. Vivas, Chosel P. Lawagon, Myoung Jun Park, Ho Kyong Shon, Neha Mittal, In Wook Nah, Hern Kim, and Wook Jin Chung. 2015. "Macroporous Flexible Polyvinyl Alcohol Lithium Adsorbent Foam Composite Prepared via Surfactant Blending and Cryo-

Desiccation." *Chemical Engineering Journal* 280 (November): 536–48.
https://doi.org/10.1016/j.cej.2015.05.107.

Park, Myoung Jun, Grace M. Nisola, Arnel B. Beltran, Rey Eliseo C. Torrejos, Jeong
Gil Seo, Seong Poong Lee, Hern Kim, and Wook Jin Chung. 2014. "Recyclable
Composite Nanofiber Adsorbent for Li+ Recovery from Seawater Desalination
Retentate." *Chemical Engineering Journal* 254 (October): 73–81.
https://doi.org/10.1016/j.cej.2014.05.095.

Pulido, Ruth, Nelson Naveas, Raúl J.Martín-Palma, Teófilo Graber, Iván Brito, Jacobo
Hernández-Montelongo, and Miguel Manso Silván. 2022. "Experimental and
Density Functional Theory Study of the Li+ Desorption in Spinel/Layered
Lithium Manganese Oxide Nanocomposites Using HCl." *Chemical Engineering
Journal* 441 (August). https://doi.org/10.1016/j.cej.2022.136019.

Qian, Fangren, Bing Zhao, Min Guo, Zhiqiang Qian, Zhijian Wu, and Zhong Liu.
2020. "Trace Doping by Fluoride and Sulfur to Enhance Adsorption Capacity of
Manganese Oxides for Lithium Recovery." *Materials & Design* 194 (September):
108867. https://doi.org/10.1016/j.matdes.2020.108867.

Recepoğlu, Yaşar K., Nalan Kabay, İdil Yılmaz-Ipek, Müşerref Arda, Mithat Yüksel,
Kazuharu Yoshizuka, and Syouhei Nishihama. 2018. "Elimination of Boron and
Lithium Coexisting in Geothermal Water by Adsorption-Membrane Filtration
Hybrid Process." *Separation Science and Technology (Philadelphia)* 53 (6): 856–
62. https://doi.org/10.1080/01496395.2017.1405985.

Roobavannan, Sharaniya, Saravanamuthu Vigneswaran, and Gayathri Naidu. 2020.
"Enhancing the Performance of Membrane Distillation and Ion-Exchange
Manganese Oxide for Recovery of Water and Lithium from Seawater." *Chemical
Engineering Journal* 396 (September). https://doi.org/10.1016/j.cej.2020.125386.

Siekierka, Anna. 2020. "Lithium Iron Manganese Oxide as an Adsorbent for
Capturing Lithium Ions in Hybrid Capacitive Deionization with Different
Electrical Modes." *Separation and Purification Technology* 236 (April).
https://doi.org/10.1016/j.seppur.2019.116234.

Sing, K. S. W. 1985. "Reporting Physisorption Data for Gas/Solid Systems with
Special Reference to the Determination of Surface Area and Porosity

(Recommendations 1984)." *Pure and Applied Chemistry* 57 (4): 603–19.
https://doi.org/10.1351/pac198557040603.

Vanessa L. Gonçalves, Mauro C. M. Laranjeira, Valfredo T. Fávere. n.d. "Effect of
Crosslinking Agents on Chitosan Microspheres in Controlled Release of
Diclofenac Sodium."

Wang, Hongshuang, Jinjie Cui, Mingli Li, Yafei Guo, Tianlong Deng, and Xiaoping
Yu. 2020. "Selective Recovery of Lithium from Geothermal Water by EGDE
Cross-Linked Spherical CTS/LMO." *Chemical Engineering Journal* 389 (June).
https://doi.org/10.1016/j.cej.2020.124410.

Wang, Shulei, Xin Chen, Ying Zhang, Yang Zhang, and Shili Zheng. 2018. "Lithium
Adsorption from Brine by Iron-Doped Titanium Lithium Ion Sieves."
Particuology 41 (December): 40–47. https://doi.org/10.1016/j.partic.2018.02.001.

Xing, Wenle, Jie Liang, Wangwang Tang, Guangming Zeng, Xiangxi Wang,
Xiaodong Li, Longbo Jiang, et al. 2019. "Perchlorate Removal from Brackish
Water by Capacitive Deionization: Experimental and Theoretical Investigations."
Chemical Engineering Journal 361 (April): 209–18.
https://doi.org/10.1016/j.cej.2018.12.074.

Xu, Xin, Yongmei Chen, Pingyu Wan, Khaled Gasem, Kaiying Wang, Ting He,
Hertanto Adidharma, and Maohong Fan. 2016. "Extraction of Lithium with
Functionalized Lithium Ion-Sieves." *Progress in Materials Science*. Elsevier Ltd.
https://doi.org/10.1016/j.pmatsci.2016.09.004.

Zandvakili, Saeid, and Mohammad Ranjbar. 2018. "Preparation and Characterisation
of Lithium Ion Exchange Composite for the Recovery of Lithium from Brine."
*Mineral Processing and Extractive Metallurgy: Transactions of the Institute of
Mining and Metallurgy* 127 (3): 176–81.
https://doi.org/10.1080/03719553.2017.1334983.

Zavahir, Sifani, Tasneem Elmakki, Mona Gulied, Zubair Ahmad, Leena Al-Sulaiti, Ho
Kyong Shon, Yuan Chen, Hyunwoong Park, Bill Batchelor, and Dong Suk Han.
2021. "A Review on Lithium Recovery Using Electrochemical Capturing
Systems." *Desalination* 500 (December 2020).
https://doi.org/10.1016/j.desal.2020.114883.

Zhang, Xiaoxian, Yue Niu, Feng Xue, Jianhong Gao, Xiaolei Zhu, and Shengui Ju. 2021. "Preparation and Evaluation of Porous H1.6Mn1.6O4@chitosan Pellet for Li+ Extraction." *Korean Journal of Chemical Engineering* 38 (10): 2141–49. https://doi.org/10.1007/s11814-021-0862-9.

Zhao, Kaiyu, Bojia Tong, Xiaoping Yu, Yafei Guo, Yingchun Xie, and Tianlong Deng. 2022. "Synthesis of Porous Fiber-Supported Lithium Ion-Sieve Adsorbent for Lithium Recovery from Geothermal Water." *Chemical Engineering Journal* 430 (February). https://doi.org/10.1016/j.cej.2021.131423.

Zhu, Guiru, Pan Wang, Pengfei Qi, and Congjie Gao. 2014. "Adsorption and Desorption Properties of Li+ on PVC-H1.6Mn1.6O4 Lithium Ion-Sieve Membrane." *Chemical Engineering Journal* 235 (January): 340–48. https://doi.org/10.1016/j.cej.2013.09.068.